

Monitoring of the Elgin Rig Leak using the FAAM Atmospheric Research Aircraft

Stephen Mobbs, Stéphane Bauguitte, Axel Wellpott, Ralph Burton, James Lee,
Alastair Lewis and Shalini Punjabi

December 2012

Final report of the National Centre for Atmospheric Science on the six flights conducted during March-August 2012 in support of TOTAL's response to the leak at the Elgin gas platform.



Contact details:

Professor Stephen Mobbs
National Centre for Atmospheric Science
School of Earth and Environment
University of Leeds
Leeds LS2 9JT
UK
Email: s.d.mobbs@ncas.ac.uk
Tel: +44 113 343 5158



Contents

1	Summary	1
2	Background	1
3	Mission Planning	1
3.1	Schedule of Events	1
3.2	Flight Planning	2
3.3	Safety Case	2
4	Scientific Background and Methodology	2
4.1	Non-methane Hydrocarbons and Other Organic Emissions	2
4.2	Aircraft Measurements	2
4.2.1	Fast Greenhouse Gas Analyzer	3
4.2.2	Whole Air Sampling	4
4.2.3	Sample Averaging	5
4.2.4	Chemical Analysis Methods	5
4.2.5	Higher hydrocarbon analysis	6
4.3	Methane Flow Rate Estimation	6
4.3.1	Method 1: Fully Mixed Layer	7
4.3.2	Method 2: Gaussian Fitting in the Vertical	7
4.3.3	Fitting Methods and Error Analysis	8
4.4	Dispersion Modelling	9
4.4.1	Post-flight Dispersion Modelling	9
5	Aircraft Flights and Results	14
5.1	Flight B688: 30 March 2012	14
5.1.1	Meteorology	14
5.1.2	Measurements	15
5.2	Flight B689: 3 April 2012	17
5.2.1	Meteorology	17
5.2.2	Measurements	18
5.3	Flight B690: 17 April 2012	21
5.3.1	Meteorology	21
5.3.2	Measurements	22
5.4	Flight B691: 24 April 2012	24
5.4.1	Meteorology	24
5.4.2	Measurements	25
5.5	Flight B693: 4 May 2012	27
5.5.1	Meteorology	27
5.5.2	Measurements	28
5.6	Flight B727: 15 August 2012	30
5.6.1	Meteorology	30
5.6.2	Measurements	31
5.7	Methane Flow Rate Results and Discussion	32
5.8	Analysis of Non-methane Hydrocarbon and Other Organic Emissions	34
5.8.1	Results	34
5.8.2	Atmospheric Chemistry impacts	36
6	Summary & Recommendations	36
6.1	Summary of Results	36
6.1.1	Flow rate	36
6.1.2	Whole Air Samples and Non-methane Hydrocarbons	36
6.1.3	HYSPLIT Dispersion Modelling	37
6.2	Lessons learned	37
6.3	Future capability	37
7	Acknowledgments	38
	References	39

1 Summary

This report describes the work carried out by the National Centre for Atmospheric Science (NCAS) in support of TOTAL during the gas leak at the Elgin platform during March-May 2012. It describes measurements of the leaking gas plume made using the large atmospheric research aircraft of the Facility for Airborne Atmospheric Measurements (FAAM). These measurements included methane and non-methane hydrocarbons. Quantitative analysis of the methane data is described, leading to estimates of the total gas flow rate of the leak. Details of the composition of the leaking gas was obtained using laboratory analysis of air samples obtained in flight. The report also describes dispersion modelling which both provided the basis of the safety case for flying through the Elgin leak plume and provided an assessment of the total exposure to methane from the leak.

This work has enabled recommendations to be developed for enhancing the response to any future incident of a similar nature. These recommendations are listed in §6.2.

2 Background

The Facility for Airborne Atmospheric Measurements (FAAM) manages a large atmospheric research aircraft. The aircraft is a highly modified BAe-146 four-engined jet aircraft. FAAM is a collaboration of the Natural Environment Research Council (NERC) and the Met Office. The NERC part of the collaboration comes within the National Centre for Atmospheric Science (NCAS). NCAS is one of NERC's six research centres, providing national capability, infrastructure, expertise, science leadership, coordination and research in atmospheric science (including weather, atmospheric chemistry and climate).

Information concerning the FAAM aircraft and its instruments is given in §4.2. The aircraft is owned by BAe Systems and operated by Directflight Ltd.

When the Elgin has leak was first detected, the FAAM aircraft was already prepared for flights to measure methane in northern Scandinavia as part of a NERC project (MAMM: Methane and other greenhouse gases in the Arctic – Measurements, process studies and Modelling). Initially, there were two motivations for a FAAM response:

- As a test of the methane measuring capability, in support of the MAMM project.
- As a potential civil contingencies response (the Met Office is tasked by Government with leading airborne atmospheric measurements as part of civil contingency requirements).

Two flights were planned. It was soon established that there was no requirement for a civil contingencies response and at that time the Met Office handed leadership of the work to NCAS, where the majority of the atmospheric chemistry expertise within the FAAM consortium is located. At that time, TOTAL contacted NCAS in order to discuss cooperation. Discussions quickly led to a series of contracts for FAAM flights to assist TOTAL in its response to the leak. This report details the findings of those flights and other associated research carried out by NCAS.

3 Mission Planning

3.1 Schedule of Events

TOTAL first reported a gas leak following an operation on well G4 on the wellhead platform at the Elgin gas field on 25 March 2012. The National Centre for Atmospheric Science (NCAS) supported the TOTAL response to the leak with flights of the Facility for Airborne Atmospheric Measurements (FAAM) BAe-146 aircraft on the following dates:

- 30 March;
- 3 April;
- 17 April;
- 24 April and
- 4 May.

TOTAL was able to announce that the leak had stopped on 16 May, following a successful intervention which involved pumping heavy mud into the leaking well. The intervention operation began on May 15 and the leak was stopped 12 hours later. In order to confirm that the leak had stopped, NCAS undertook one more flight on the following date:

- 15 August.

3.2 Flight Planning

Each flight was initiated either by a decision by NCAS (in the cases of the first two flights) or a request by TOTAL (in the cases of the remaining flights). Not later than 12:00 noon on the day before each flight, a sortie brief was submitted by NCAS to Directflight. These sortie briefs included the outline flight plan, the scientific objectives, an assessment of the meteorological forecasts and dispersion predictions. TOTAL were offered opportunities to comment on each sortie brief. Based on the sortie briefs, Directflight developed the detailed flight plans, permissions and safety cases. At the same time, FAAM and NCAS assembled an appropriate team of scientists, drawn from FAAM, NCAS and the Met Office, to act as crew for the flight. Flights typically required 7-10 scientists and were planned for up to five hours.

3.3 Safety Case

In order to fly the Elgin missions, the operator of the FAAM aircraft, Directflight Ltd, had to agree a Safety Management System, eliminating the possibility of flying into conditions harmful to the aircraft, its crew or passengers. In outline, this involved using best previous estimates of composition and emission rates of the leak, coupled with use of a dispersion model. Dispersion predictions were required by Directflight 24 hours in advance of a flight, allowing the operator to establish that the proposed flight plan did not involve encountering concentrations above previously agreed limits. A “turn away” detection value of 40 ppm CH₄ was established, which was 20 times any forecast concentration likely to be present and 100 times lower than any possibly dangerously combustible concentration of the worst case gas mixture.

The safety case also required the aircraft to climb and move to a safer area if H₂S be detected by human or instrument sensing. This did not occur.

4 Scientific Background and Methodology

4.1 Non-methane Hydrocarbons and Other Organic Emissions

Non-methane hydrocarbons (NMHCs) are class of trace compound found throughout the troposphere. Whilst typically present at mixing ratios in the parts per billion and trillion range, they exert significant influence over the oxidizing capacity of the troposphere, the lifetime of methane and the formation of tropospheric ozone (Houweling et al. (1998)). They play a central role in controlling the lifetime (τ) of OH and can influence its rate of production via ozone + alkene reaction. Some species are also now implicated in the generation of secondary oxidation products, which can aid the formation of secondary aerosols (Hallquist et al. (2009) and references therein). NMHCs are released from a wide range of biogenic and anthropogenic sources. Most individual NMHCs have a mix of sources, with isoprene (the largest global emission by mass) being the prime exception with emissions almost exclusively from terrestrial vegetation. Incomplete combustion is generally the largest individual anthropogenic source of NMHCs, including petrol and diesel engines, static power generation and the burning of wood and coal for heating and cooking. Substantial anthropogenic emissions arise from the extraction, refining and transportation of petrochemicals. Condensate gases released from natural gas extraction are typically dominated by light saturated hydrocarbons such as ethane and propane but with contributions from other hydrocarbons as large as C₁₂. As a class of compound, NMHCs have wide range of atmospheric lifetimes, from a few minutes to several months. The range of lifetimes of NMHCs together with their disparate regional sources, have a major impact in defining their global distribution (Atkinson (1994)).

4.2 Aircraft Measurements

This FAAM BAe-146 aircraft is a modified BAe-146-300 aircraft which carries core and optional instruments for measuring the atmosphere. Core instruments cover a range of basic atmospheric measurements including thermodynamic properties, wind, turbulence and some chemical species. These are provided by FAAM as part of the facility. Optional instruments include sophisticated cloud and aerosol facilities and remote sensing using LIDAR or radiometers. Use of these instruments generally involves the agreement of the instrument owner.

Details of most FAAM instruments can be found on the FAAM web-site: <http://www.faam.ac.uk>. Wind and turbulence are provided using a five-port pressure measurement system in the aircraft radome, combined with two scientific static ports located symmetrically on either side of the aircraft. Of greatest relevance to the work reported here are the systems for fast methane measurement and for obtaining air samples for laboratory analysis. These are described below.

4.2.1 Fast Greenhouse Gas Analyzer

A Fast Greenhouse Gas Analyser (FGGA) model RMT-200 from Los Gatos Research Inc is installed on the FAAM BAe-146 aircraft as part of the core chemistry instrumentation. This instrument and its predecessor model, the Fast Methane Analyser (FMA), have previously been successfully used for ground based mole fraction and eddy covariance flux measurements. The FAAM system is now well tested, having been central to three recent major campaigns: BORTAS (Quantifying the impact of BOREal forest fires on Tropospheric oxidants over the Atlantic using Aircraft and Satellites – a boreal forest fire plume experiment in Canada), MAMM (Methane and other greenhouse gases in the Arctic – Measurements, process studies and Modelling – an experiment to investigate methane sources at northern high latitudes) and SAMBBA (South American Biomass Burning Analysis – a campaign investigating biomass burning plumes in the Brazilian Amazon basin).

The measurement set-up, optimisation, laboratory testing, in-flight calibration methodologies, data processing and quality control are fully described in O’Shea et al. (2013). The instrument uses a technique known as off axis-integrated cavity output spectroscopy (OA-ICOS), which has been described in detail by Paul et al. (2001) and Baer et al. (2002). The FGGA uses two near infrared distributed feedback diode lasers, one to probe a CO₂ absorption line near 1.603 μ m and the other to probe CH₄ and H₂O absorption lines near 1.651 μ m. The instrument acquisition rate can be up to 10 Hz, but is routinely operated at 1 Hz on the FAAM aircraft. Sample air is continuously pumped through the instrument detector cell, which comprises a 0.4 litre optical absorption cavity consisting of two high reflectivity mirrors (reflectivity, $R > 0.9999$). For airborne operation, the sample cavity pressure is held at a constant value of 50 Torr over the range of inlet pressures that are experienced during flight (1000 to 250 hPa). The instrument inlet consisted of a ~7m long 3/8" OD PFA Teflon inlet for the first four Elgin missions (B688-B691), connected to the aircraft starboard ram air sampling pipe. This was subsequently upgraded to a dedicated window mounted rearward facing 3/8" OD stainless steel tube. Figure (1) shows a schematic of both the instrument sample flow system and the calibration gas system. With the internal throttle valve closed, the combination of the external diaphragm vacuum pump (N920APDCB, KNF Neuberger, UK) and of the internal electronic pressure controller, allowed the cavity pressure to be maintained at 50.00 ± 0.07 Torr with a sample volumetric flow rate of ~0.76 ccm over an altitude range of surface to 8200 m.

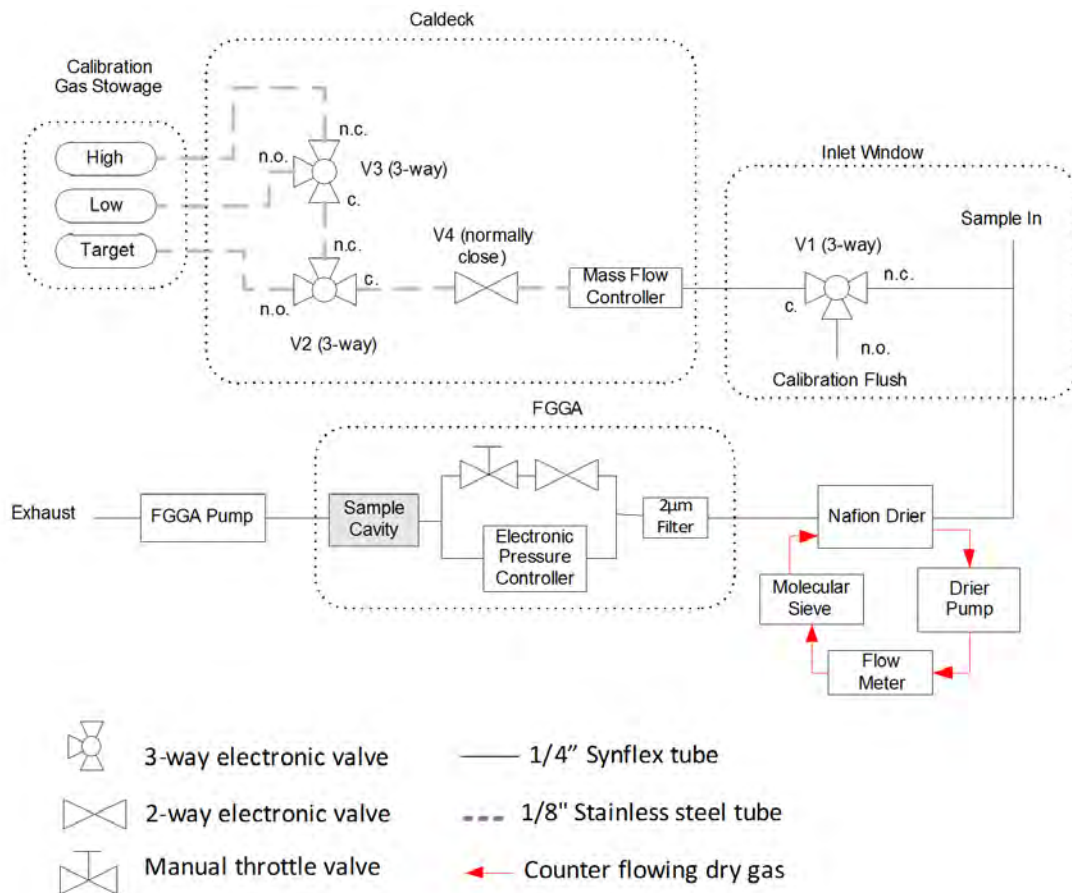


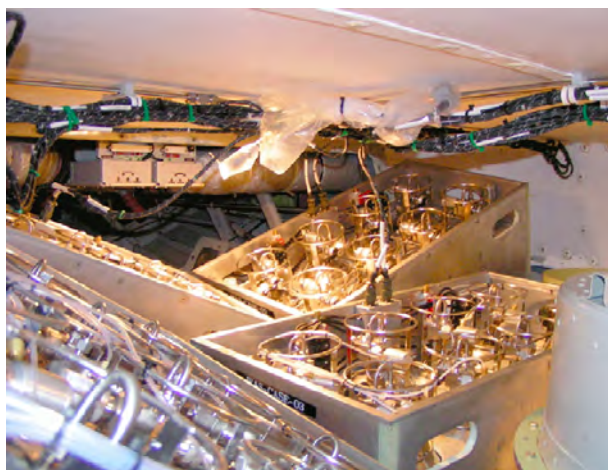
Figure 1: The sample and calibration air flow through the CO₂ and CH₄ system.

The instrument inlet, sample lines and flow components are optimised to achieve the shortest possible response time to ambient gas mole fraction changes, allowing high spatial resolution measurements required for the identification of sharp, near source plumes. During the Elgin rig flights the high spatial resolution was necessary both in order to resolve the narrow plume close to the source and also to trigger the collection of whole air samples while penetrating plumes. The total response time of the system is a combination of the time taken to travel through the lines from the aircraft's inlet to the sample cavity plus the time taken for the instrument to respond fully to the change in mole fraction. Response times were measured and assessed for both inlet configurations. At 1007 hPa inlet pressure, the inlet #1 has a lag time of 20.8 ± 1.0 s. This lag time is responsible for the decoupling of plume transects showed for instance in §5.1.2 (Figures 13 and 15). At 1007 hPa inlet pressure, the improved inlet #2 lag time was 4.0 ± 1.0 s, and the FGGA cavity's e-folding time was 1.4 ± 0.1 s. The response time was found to improve marginally with altitude, e.g. at 287 hPa inlet pressure, the inlet #2 lag time was 2.0 ± 1.0 s and the e-folding time was 1.5 ± 0.1 s.

Customisation of the FGGA provides for in-flight calibration for instrument sensitivity/stability checks, to allow post-processing of dry air mole fractions traceable to greenhouse gas scales of the Global Atmospheric Watch programme, World Meteorological Organisation (WMO). Instrumental performance based on analysis of in-flight (known) target concentration measurements is as follows: 1 Hz accuracy 0.07 ± 2.48 ppbv for CH_4 and -0.06 ± 0.66 ppmv for CO_2 .

4.2.2 Whole Air Sampling

Non-methane hydrocarbons are sampled using the whole air sampling (WAS) system fitted to the FAAM BAe-146 research aircraft. The WAS system consists of sixty-four silica passivated stainless steel canisters of three litre internal volume (Thames Restek, Saunderton UK) fitted in packs of 8, 9 and 15 canisters to the rear lower cargo hold of the aircraft. The WAS system is a mature and well-tested instrument on the aircraft, first installed in 2004, and is used regularly to sample a range of stable trace gases not limited to hydrocarbons, but also including halocarbons, organic nitrates, sulphur compounds, greenhouse gases and stable isotopes. Figure (2a) below shows some of the WAS canister packs installed in the FAAM aircraft hold.



(a) WAS system installed in the hold of the FAAM aircraft.



(b) WAS sample pumps and pressure reliefs located in the aircraft main cabin.

Figure 2: The FAAM aircraft WAS system.

Each pack of canisters was connected to a 5/8 inch diameter stainless steel sample line connected in turn to an all-stainless steel assembly double-headed three phase 400 Hz metal bellows pump (Senior Aerospace, USA). Each canister was opened and closed for filling remotely via a PC interface in the main cabin, which triggered 24V dc solenoid valves that provided the actuation to open all-metal assembly diaphragm valves. This process can be completed either automatically, filling canisters at predetermined times or on user command. For the Elgin plume sampling canister filling was triggered manually. The pump drew air from the port-side sample manifold and pressurized air in to individual canisters to a maximum pressure of 3.25 bar (giving a useable sample volume for analysis of up to 9 litres).

4.2.3 Sample Averaging

WAS canisters take approximately 10 seconds to fill to 3 Atm pressure (at typical boundary layer pressures) and so they provide an averaged measure of hydrocarbon content. At a typical aircraft science speed of around 100 m s^{-1} a WAS sample is therefore an average mixing ratio over a spatial extent of 1 km. The length of sampling manifold within the aircraft creates a delay of around 10 seconds between air entering the inlet at the front of the aircraft and being available for capture in the hold. This slight delay allowed the real-time CH_4 outputs from the FGGA to be used to aid the capture plume samples with canisters. The integrated nature of the WAS means that the concentrations reported do NOT represent peak plume concentrations. However peak concentrations can be inferred assuming a constant relationship to CH_4 .

4.2.4 Chemical Analysis Methods

Air samples were analysed for non-methane hydrocarbons and other organic compounds, in the NCAS labs at the University of York, typically within 48 hours of collection. The primary analytical method used a dual channel gas chromatograph (GC) with two flame ionization detectors. This instrument resolves hydrocarbons in the carbon number range C2-C8. The full methodology is reported in Hopkins et al. (2003, 2011). Briefly, one litre samples of air were withdrawn from the sample canisters and dried using a glass condensation finger to a fixed dew point of $-30 \text{ }^\circ\text{C}$. Dried gas was pre-concentrated onto a multi-bed carbon adsorbent trap, consisting of Carboxen 1000 and Carbotrap B (Supelco), held at $-20 \text{ }^\circ\text{C}$. Following pre-concentration of one litre of sample, the carbon bed was heated to $325 \text{ }^\circ\text{C}$ at $16 \text{ }^\circ\text{C s}^{-1}$ and transferred to the GC columns in a stream of helium. The eluent was split in an approximately 50:50 ratio between an aluminium oxide (Al_2O_3 , NaSO_4 deactivated) porous layer open tubular PLOT column (50 m, $0.53 \text{ }\mu\text{m}$ id) for analysis of NMHCs and two LOWOX columns (10 m, $0.53 \text{ }\mu\text{m}$ id) in series for analysis of polar VOCs (volatile organic compounds). Both columns were supplied by Varian, Netherlands. Peak identification and calibration was made by reference to a part per billion level certified gas standard (National Physical Laboratory, ozone precursors mixture, cylinder number: D64 1613) for NMHCs. This standard and instrument has in turn been evaluated as part of the Global Atmosphere Watch programme and was within WMO data quality objectives. A relative response method was used for the calibration of OVOCs (oxygenated VOCs) in the field, with reference to propane. The response values of OVOC to propane were derived from laboratory calibration using ppm gas standard dilution and permeation methods. Detection limits for individual species were in the range 110 ppt depending on carbon number and functionalisation. The run to run reproducibility of mixing ratios is better than 0.5%; however uncertainty is around 3% due to uncertainties in the gravimetric gas standards used for calibration. Figure (3) below shows a typical instrument output chromatogram for hydrocarbons and a small number of oxygenated species.

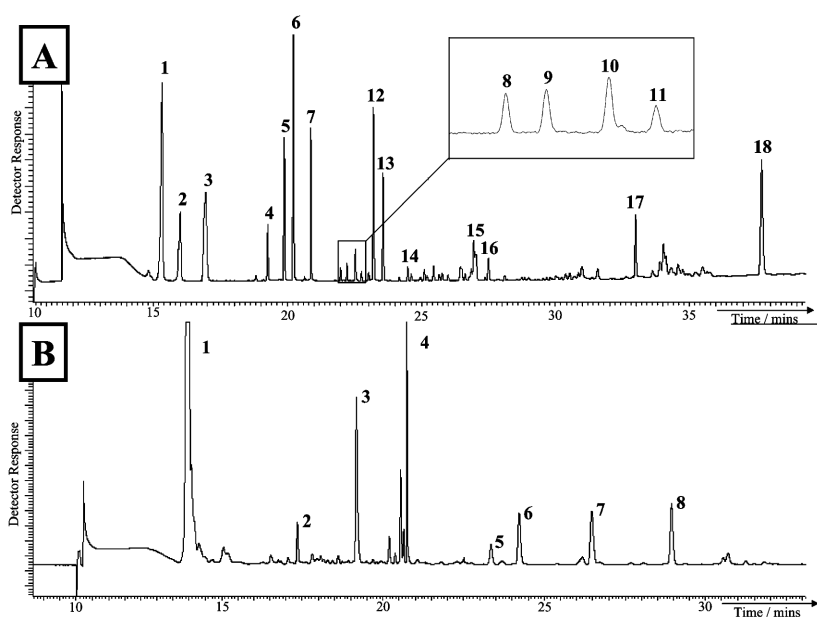


Figure 3: Typical C2-C8 hydrocarbon analysis from a WAS canister using the methods described in this report. Figure taken from Hopkins et al. (2003). Sample chromatograms produced from (A) Al_2O_3 PLOT column where 1; ethane, 3; propane, 4; propene, 5; iso-butane, 6; n-butane, 7; acetylene, 8; but-1-ene, 9; *trans*-but-2-ene, 10; iso-butene, 11; *cis*-but-2-ene, 12; iso-pentane, 13; n-pentane, 14; buta-1,3-diene, 15; 2+3-methylpentane, 16; n-hexane, 17; benzene, 18; toluene. (B) LOWOX column where 1; Aliphatic NMHCs. 2; benzene, 3; toluene, 4; acetaldehyde, 5; methanol, 6; acetone, 7; ethanol, 8; propanol.

4.2.5 Higher hydrocarbon analysis

Hydrocarbons with carbon number greater than C8 can make significant contribution to the overall OH reactivity in an air mass and can be disproportionately important in generating ozone and aerosols. The analysis of larger hydrocarbons, particularly from fossil fuel sources, is more difficult than for C2-C8 since isomeric complexity increases exponentially with carbon number. A multidimensional gas chromatography method (GCxGC) has been used here to assess >C8 NMHCs. The methodology is described in detail by Lidster et al. (2011). Briefly this uses an Agilent 7890 GC (Agilent Technologies, Wilmington, DE, USA) equipped with a Markes TT-24/7 thermal desorption unit and a flame ionisation detector operated at 100 Hz. Comprehensive GC was enabled using a fluidic modulator constructed from a gas actuated fast switching 6-port 2-way diaphragm valve (Valco Instruments Company Inc, Houston, TX, USA) with a 50µl sample loop (Thames Restek). Valve actuation was achieved using a solenoid valve and compressed air line. Decompression of the actuation line results in the valve returning rapidly to its starting position. The sample loop is blocked at the exit so no carrier gas is vented to waste. Stainless steel tubing (5 cm, 1.5875 mm o.d. and 0.127 mm i.d.) was used to connect the valve ports to a low dead volume union which was then connected to the GC columns, injector and detector using graphite-vespel ferrules. Columns used were BPX-5 12 m × 0.15 mm × 0.25 µm d.f. primary column (a volatility based separation) and a BPX-20 (PEG) 2 m × 0.25 mm × 0.25µm d.f. (SGE) (a polarity based separation). Detection limits for individual hydrocarbons are less than 1 part per trillion for a 4 litre air sample, with run to run reproducibility of better than 2%.

4.3 Methane Flow Rate Estimation

The plume of methane and other gases is assumed to be neutrally buoyant and non-reacting (on the time and distance scales involved in the aircraft measurements). The fundamental assumption is that the plume dispersion may be modelled by a Gaussian distribution (Turner (1994)):

$$C(x, y, z) = \frac{q}{\pi\sigma_y\sigma_zU} \exp\left(-\frac{(y-y_0)^2}{2\sigma_y^2} - \frac{z^2}{2\sigma_z^2}\right). \quad (1)$$

Here q is the source strength of the leak (in kg s⁻¹), $C(x, y, z)$ is the concentration which varies in the x (downwind), y (cross-wind) and z (vertical) directions and U is the wind speed. σ_y^2 and σ_z^2 are the mean squared distances of the plume spread in the cross-wind and vertical directions (both growing with down-wind distance). The source is at $x = 0$ and $z = 0$. The reason for not taking the centre-line of the plume to necessarily be at $y = 0$ is that during cross-plume aircraft flights, the cross-wind position y_0 of the plume is to be determined from the measurements. The assumptions underlying Eq. (1) are:

1. The wind velocity does not exhibit strong shear in the vertical. This includes both changes in speed U and direction.
2. The height above the sea surface of the source may be neglected. Although relatively straightforward to include, other uncertainties in the measurements of the Elgin plume make this parameter negligible.
3. Similarly, any effect on the vertical mixing of structural down-wash from the rig structure is not detectable at the levels of uncertainty exhibited.
4. There is negligible vertical restriction of mixing by capping inversions or the boundary-layer top.

Assumption (4) is clearly not always valid. It is relatively straightforward, from a theoretical point of view, to account for a restricted mixing height H (Turner (1994)):

$$C(x, y, z) = \frac{q}{\pi\sigma_y\sigma_zU} \exp\left(-\frac{(y-y_0)^2}{2\sigma_y^2}\right) \left[\exp\left(-\frac{z^2}{2\sigma_z^2}\right) + \exp\left(-\frac{(z+2H)^2}{2\sigma_z^2}\right) + \exp\left(-\frac{(z-2H)^2}{2\sigma_z^2}\right) \right]. \quad (2)$$

However, fitting of Eq. (2) to experimental data with large uncertainties is not feasible. Mathematically, fitting is relatively straightforward but in practice it is not possible to distinguish reliably between the effect of an elevated inversion and a general reduction in vertical spreading σ_z . Far down-wind, in the presence of an elevated inversion which strongly inhibits mixing above height H , the pollutant is thoroughly mixed below the inversion and further mixing results only in horizontal spreading. Then a much simpler Gaussian plume model may be used (Turner (1994)):

$$C(x, y) = \frac{q}{\sqrt{2\pi}\sigma_yUH} \exp\left(-\frac{(y-y_0)^2}{2\sigma_y^2}\right). \quad (3)$$

Based on the above theoretical considerations, a measurement strategy has been used which follows closely that used by (Ryerson et al. (2011)) during the 2010 Deepwater Horizon spill in the Gulf of Mexico. The basis of the method is to sample the cross-wind structure of the plume using repeated aircraft passes across the plume down-wind of the source. The repeated cross-plume sampling aims to determine the cross-wind structure (σ_y, y_0) and peak concentration, plus to determine how these parameters vary in the vertical and in the down-wind direction. Two different analysis approaches have been used, determined by the outcome of these measurements. They are referred to as **Method 1** and **Method 2** in this report.

4.3.1 Method 1: Fully Mixed Layer

Method 1 is essentially that used by Ryerson et al. (2011). The approach is appropriate when:

- there exists a clear temperature inversion/elevated stable layer in atmospheric profiles revealed using dropsondes or radiosondes, and
- cross-wind transects show little decrease of concentration with height (within the uncertainties), up to the inversion level.

Assuming conditions are suitable for **method 1**, then writing Eq. (3) as

$$C(x, y) = C_0 \exp\left(-\frac{(y - y_0)^2}{2\sigma_y^2}\right) \quad (4)$$

where

$$C_0 = \frac{q}{\sqrt{2\pi}\sigma_y U H}, \quad (5)$$

best fitting of the concentration measurements to Eq. (4) is used to determine C_0, y_0 and σ_y and then the leak rate q is determined from Eq. (5), using estimates of the inversion height H from the atmospheric soundings.

4.3.2 Method 2: Gaussian Fitting in the Vertical

Method 2 is appropriate when:

- there exists no significant temperature inversions at levels where $z \leq \sigma_z$. This requires that measurements are made up to a height of at least σ_z and that no inversions are encountered up to that level.

If an inversion layer does exist, then method 2 may still be used if the measured value of σ_z is such that $\sigma_z \ll H$, where H is the mixing layer height.

Writing Eq. (1) as

$$C(x, y, z) = C_z(x, z) \exp\left(-\frac{(y - y_0)^2}{2\sigma_y^2}\right) \quad (6)$$

where

$$C_z(x, z) = C_0(x) \exp\left(-\frac{z^2}{2\sigma_z^2}\right) \quad (7)$$

and

$$C_0 = \frac{q}{\pi\sigma_y\sigma_z U}, \quad (8)$$

then C_z and σ_y may be obtained from fitting cross-plume data at fixed distance down-wind to Eq. (6). Then writing Eq. (7) in the form

$$\ln(C_z) = \ln(C_0) - \frac{z^2}{2\sigma_z^2}, \quad (9)$$

C_0 and σ_z can be obtained by plotting C_z against z^2 using data from all transect levels at a fixed downwind distance.

4.3.3 Fitting Methods and Error Analysis

Both method 1 and method 2 require fitting the Gaussian plume equation (Eq. (6) or Eq. (4)). It is first necessary to note that in the measured methane data the plume is superimposed upon a larger background concentration C_b . Hence the fitted equation needs to be written as

$$C(x, y, z) = C_b + C_z(x, z) \exp\left(-\frac{(y - y_0)^2}{2\sigma_y^2}\right). \quad (10)$$

C_b was determined from averaging data towards the ends of each straight and level aircraft run. This makes negligible contribution to the uncertainties. Suppose then that the measured data consists of n data pairs (y_i, C_i) , $i = 1 \dots n$. The aim is to determine the best values of C_z , y_0 and σ_y such that the mean square error E^2 is minimised, where

$$E^2 = \frac{1}{n} \sum_{i=1}^n \left\{ C_i - C_b - C_z \exp\left(-\frac{(y_i - y_0)^2}{2\sigma_y^2}\right) \right\}^2. \quad (11)$$

The minimisation can be performed by solving the three nonlinear equations:

$$\frac{\partial E^2}{\partial C_z} = 0; \quad (12)$$

$$\frac{\partial E^2}{\partial y_0} = 0; \quad (13)$$

$$\frac{\partial E^2}{\partial \sigma_y} = 0. \quad (14)$$

using Newton's iteration method. Due to the nonlinearity of these equations, it has been found necessary to apply strong relaxation to the iteration (typical relaxation factors of ~ 0.01) in order to ensure convergence. Convergence is therefore generally rather slow.

The uncertainties in the fitted parameters C_z , y_0 and σ_y could be determined directly from the uncertainties in the concentration and position data. However, this would lead to misleadingly small uncertainties, due to a sampling issue. Ideally, the plume behaviour would be a good fit to the model equation Eq. (10) and it would be well sampled. In practice neither is true. The Gaussian plume model is an approximation to real behaviour. Of even greater significance is that the plume model represents expected behaviour averaged over many eddy turn-over times or averaged over many realisations of the same statistically stationary plume. In contrast, the aircraft crosses the plume in a time much smaller than the eddy turn-over time and so the data from a single aircraft pass essentially represents a snapshot in time. This could be overcome by repeating each aircraft pass multiple times. This was not done during the Elgin flights, in large part because time did not allow this. Instead, the lack of fit of each individual snapshot of the plume is viewed as contributing the most significant part of the uncertainties in the fitted parameters. The issues of statistical sampling of the plume are discussed further in §6.2.

Consistent with the above approach to sources of uncertainty, the uncertainties in the fitted values of C_z , y_0 and σ_y can be determined by the method described in Press et al. (2007) as follows. Let r be one of C_z , y_0 and σ_y and let its corresponding uncertainty be Δ_r . Then

$$\Delta_r^2 = \frac{E^2}{n - 3} \sum_{i=1}^n \left(\frac{\partial r}{\partial y_i} \right)^2. \quad (15)$$

In practical implementation the derivatives $\partial r / \partial y_i$ can be determined numerically by repeatedly performing the nonlinear parameter fitting with small increments applied to each of the observed coordinates y_i . This means that the nonlinear curve fitting has to be applied not once to each data-set but for n data points it has to be applied $n + 1$ times.

Method 2 requires that σ_z to be determined from fitting to Eq. (9). This is much more straightforward than the nonlinear fitting in the horizontal since the relationship between $\ln(C_z)$ and z^2 is linear. Standard least squares fitting gives the parameters C_0 and σ_z and the corresponding uncertainties may be determined from the standard errors (Press et al. (2007)).

An additional potential source of error would arise if there were a significant deviation between the wind direction and the perpendicular to the aircraft track. This would introduce an additional factor of the cosine of the deviation angle into Eq. (5) and (8). However, analysis of all the flights has shown that the change to the estimated flow rate was never greater than 3%, which is much smaller than other uncertainties. This factor has not been included in the analysis.

4.4 Dispersion Modelling

Dispersion modelling in support of the aircraft flights has been carried out using the HYSPLIT Lagrangian dispersion model from NOAA (Draxler and Hess (1997, 1998); Draxler (1999)). There were two separate motivations:

1. Pre-flight calculations of the expected distribution of methane as part of the flight planning (§3.2) and flight safety case (§3.3).
2. Post flight calculations for interpretation purposes.

4.4.1 Post-flight Dispersion Modelling

HYSPLIT model simulations were carried out using meteorological fields from the US National Centre for Environmental Prediction Global Forecast System (NCEP-GFS). NCEP GFS data are high resolution (0.5 degree latitude and longitude and 3 hours temporally). The model was run for each day between 25th March 2012 at 18:00 UTC and 16th May 2012 at 18:00 UTC. For each day, a 72-hour dispersion forecast was produced and the concentration at 72 hours after initialisation was recorded. Then, a time average of these 72-hour concentration distributions was produced. Thus, dispersion predictions were produced valid for the period 28th March 18:00 UTC until 19th May 2012 18:00 UTC. Calculations have only been made for methane and assume that the methane is long-lived (lifetime much greater than the 3 day model runs). The source strength was allowed to vary temporally using an interpolated time series from the measured flow rate in §5.7.

The methane concentration fields constructed from averaging all 53 days as described above are shown in Figure (4) for a range of height bands. Several features are noteworthy. At all levels, the majority of the methane was distributed mainly to the south of the source. Low levels of methane travelled as far as mainland UK (principally the Humber Estuary, the North Norfolk Coast and the North Yorkshire coast) and continental Europe (Netherlands). The highest levels of concentration, however, appear to be confined to a rectangular box that extended from 56° N to 57° N and from 1° E to 3° E. This confinement is true at all levels. Above approximately 1 km above sea level the concentrations were negligible.

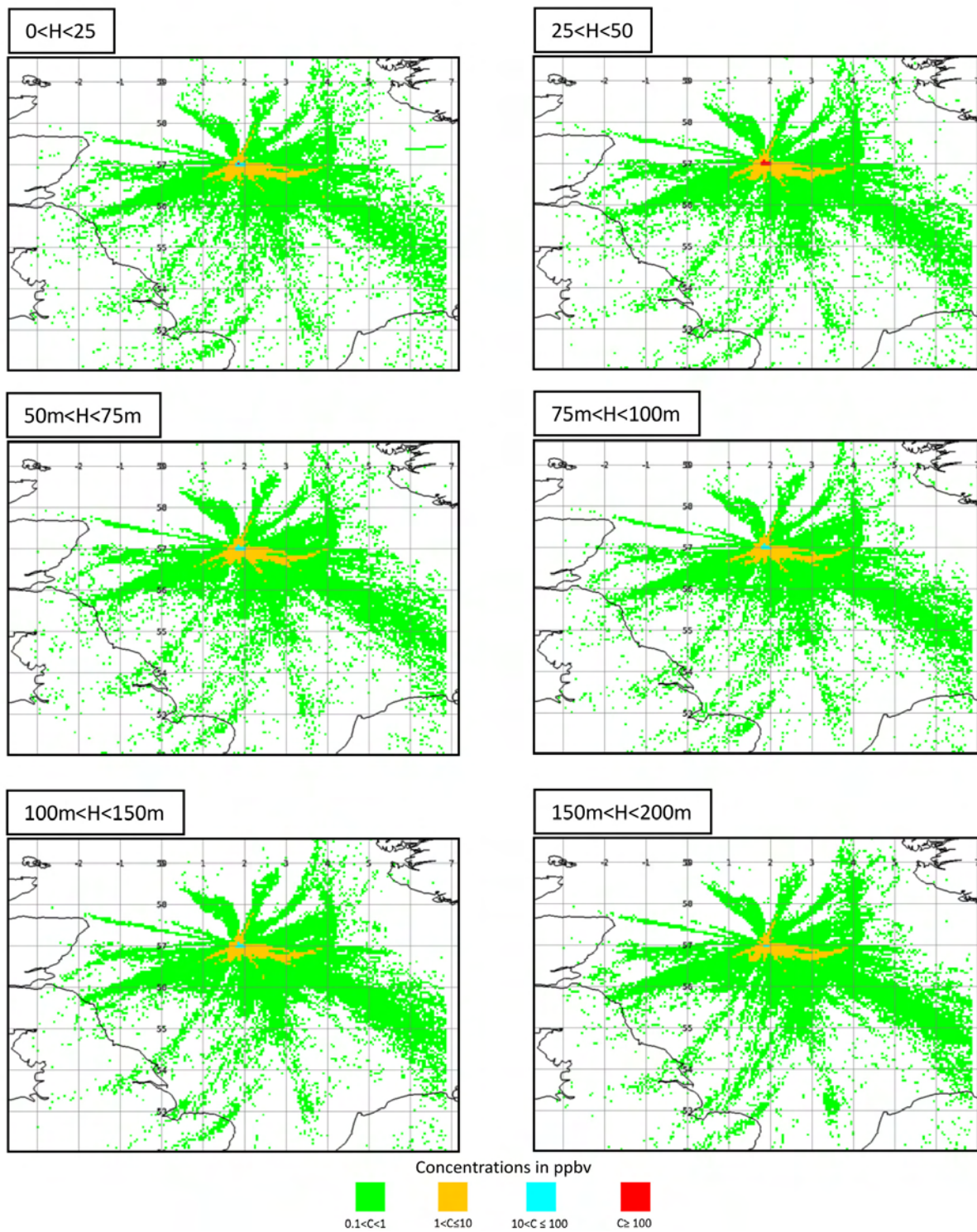


Figure 4: (a) HYSPLIT calculation of methane concentration averaged over the period 28th March 2012 at 18:00 UTC to 19th May 2012 at 18:00 UTC. Each figure shows concentration averaged over the height range indicated at the top of the plot.

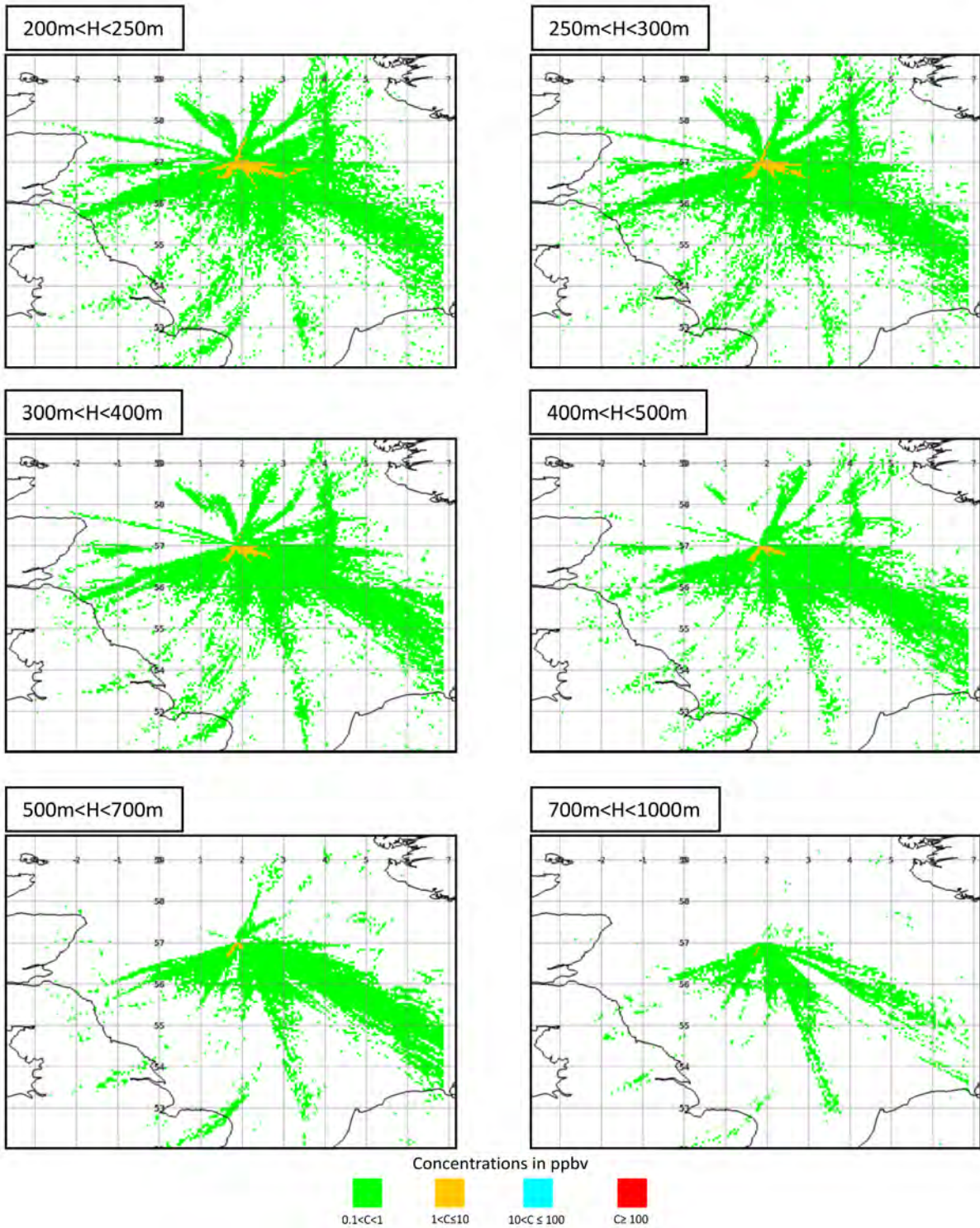


Figure 4(b) HYSPLIT calculation of methane concentration averaged over the period 28th March 2012 at 18:00 UTC to 19th May 2012 at 18:00 UTC. Each figure shows concentration averaged over the height range indicated at the top of the plot.

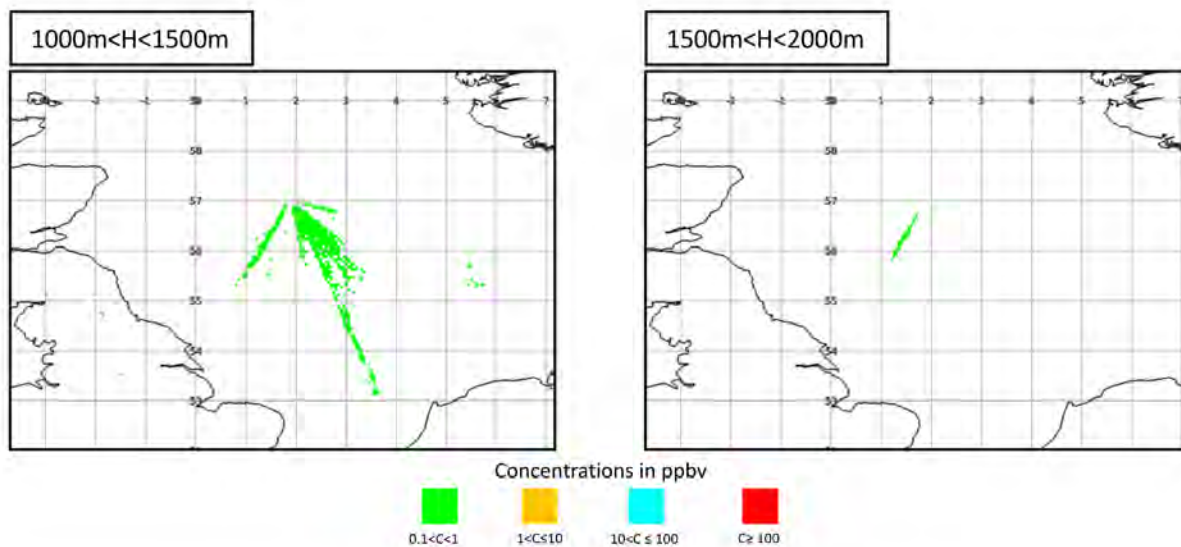


Figure 4(c) HYSPLIT calculation of methane concentration averaged over the period 28th March 2012 at 18:00 UTC to 19th May 2012 at 18:00 UTC. Each figure shows concentration averaged over the height range indicated at the top of the plot.

Figure (5) shows the wind rose (calculated from the NCEP-GFS data) for the same period. The predominance of north-westerly winds is evident.

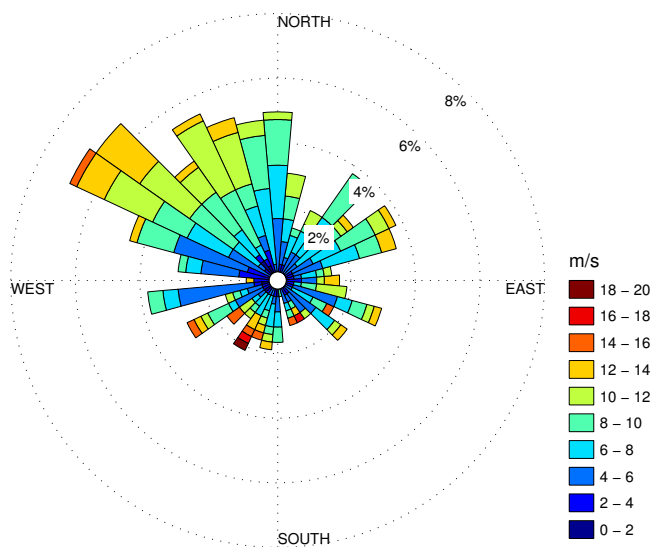


Figure 5: Wind rose calculated from NCEP-GFS data for the period 28th March to 19th May 2012.

In §5.8.2 it is noted that there were some suggestions of the Elgin plume being detected far from the North Sea (e.g. at the Jungfraujoch Observatory in Switzerland). Dispersion modelling can be used to investigate whether this is plausible. Figure (6) shows HYSPLIT results, calculated as above, but broken down by week and displayed over a larger domain (at lower resolution). There is evidence of the plume reaching Switzerland (at very low concentrations) during periods 28th March to 10th April and 9th to 19th May.

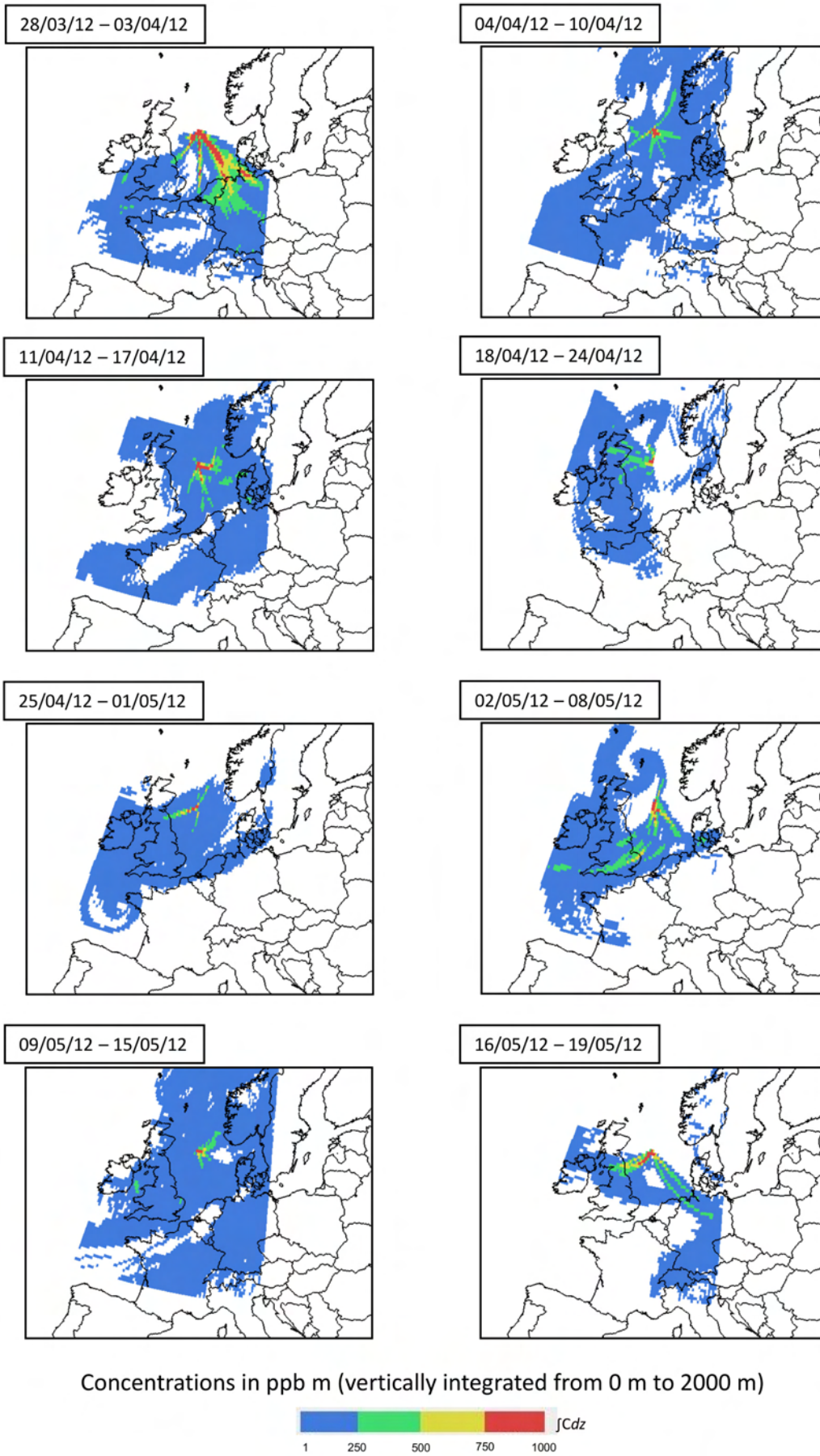


Figure 6: Weekly HYSPLIT calculations of methane concentration over a large domain.

5 Aircraft Flights and Results

5.1 Flight B688: 30 March 2012

5.1.1 Meteorology

The take-off time was 10:06 UTC. Figures (7) to (10) show the Met Office surface analysis chart and three satellite images for the period of the flight. A large and slow moving anticyclone was centred to the west of Ireland with a north-westerly wind over most of the North Sea and weak, slow-moving fronts over the eastern North Sea. The visible satellite images show clear conditions over the western North Sea and broken, low-level cloud over and to the west of the Elgin platform. This pattern did not change significantly during the flight and cloud was sufficiently broken to allow descent to low level in the Elgin region.

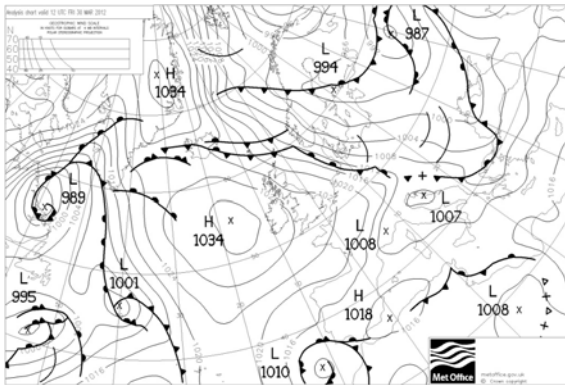


Figure 7: Surface analysis chart from the Met Office for 12:00 UTC on 30 March 2012.

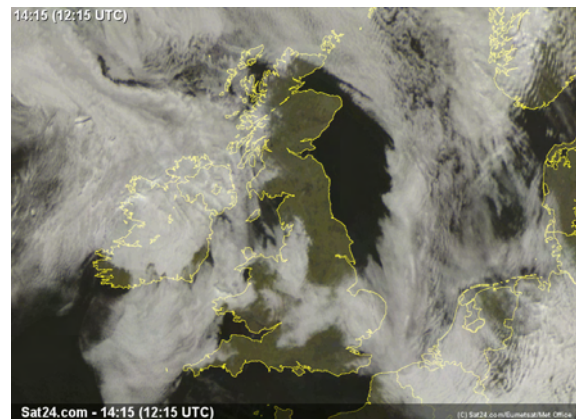


Figure 8: Meteosat visible satellite image for 12:15 UTC on 30 March 2012.

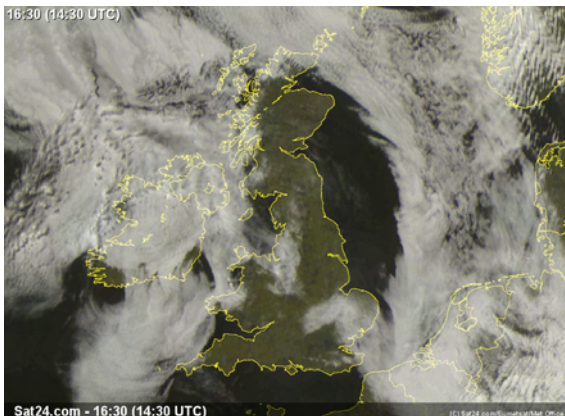


Figure 9: Meteosat visible satellite image for 14:30 UTC on 30 March 2012.

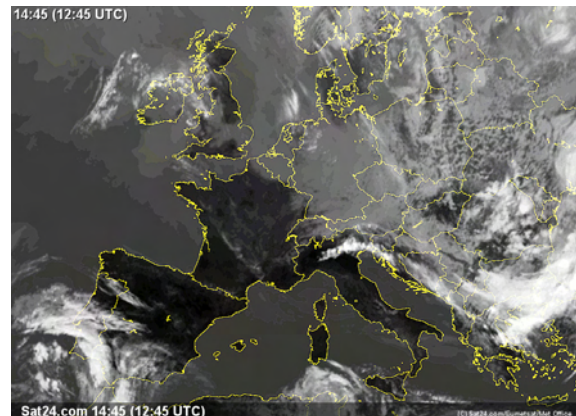


Figure 10: Meteosat infrared satellite image for 12:45 UTC on 30 March 2012.

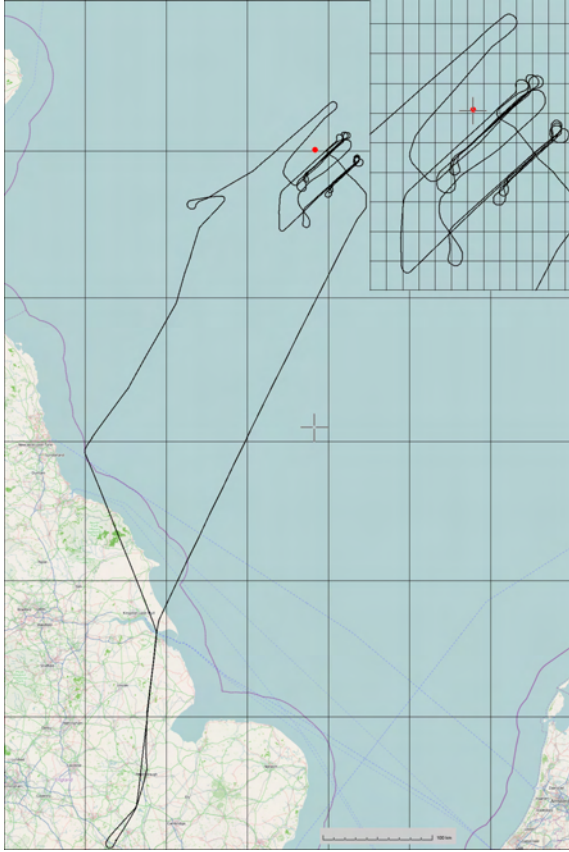


Figure 11: Flight track for flight B688 on 30 March 2012. The position of the Elgin rig is marked in red.

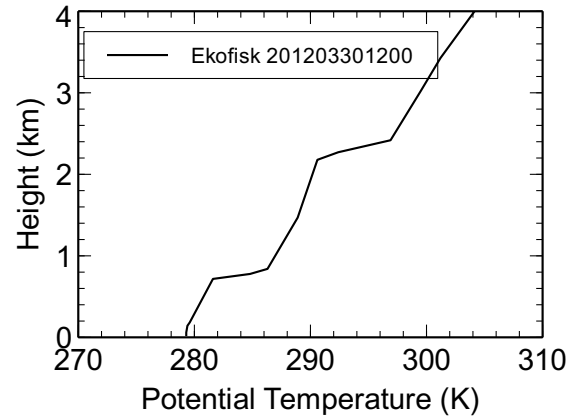
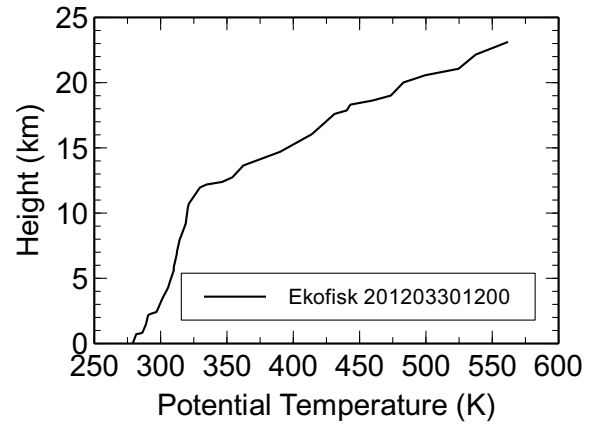


Figure 12: Atmospheric profiles from a radiosonde launched from the Ekofisk platform (SE of Elgin) at 12:00 UTC on 30 March 2012.

5.1.2 Measurements

The flight track is shown in Figure (11). Initially two passes were made across the line of the expected plume but around 10 nm upwind of the Elgin rig. These provided background methane concentrations. The aircraft was then repositioned downwind of the rig and repeated passes were made across the plume at two distances (approximately 5 nm¹ and 15 nm) from the rig. During operations downwind of the rig air samples were also collected for later analysis. Mean wind speeds were in the range 12-20 ms⁻¹.

Figures (13) and (14) show the measured and fitted (using the method described in §4.3) methane concentrations across the plume at approximately 5 nm downwind. Figures (15) and (16) show the same quantities measured 15 nm downwind. At 5 nm the plume is very clearly defined and the corresponding fitted profiles are excellent fits. At 15 nm the plume has become more broken and indeed for one of the passes it appears to have split into two separate plumes.

Figures (17) and (18) show the variation of the fitted parameters σ_y and C_z (see Eq. (6)) with height at each of the two downwind stations. There is no systematic variation of σ_y with height but it does increase with distance downwind (as expected). At both stations the plume peak concentration decreases with height. The decrease is evidence for the plume not being fully mixed up to an inversion level. For this flight, which was made with a short preparation period, no dropsonde was launched. We do however have available a profile from a radiosonde launched at the time of the flight from the nearby Ekofisk rig. This is shown in Figure (12). There is clear evidence of a temperature inversion at around 800 m. However the fitted plume parameters suggest that mixing has not occurred up to this level, even at 15 nm downwind. The method 2 of §4.3 has therefore been used for flow rate estimation. All flow rate results are shown in §5.7.

¹nautical miles

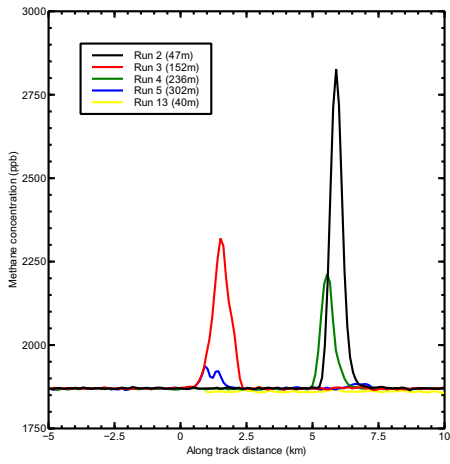


Figure 13: Raw methane measurements, flight B688, 5 nm downwind.

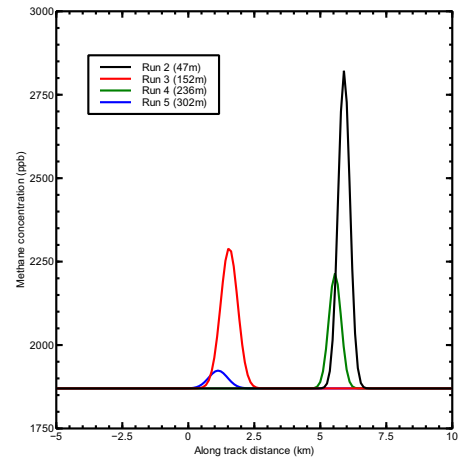


Figure 14: Fitted methane profiles, flight B688, 5 nm downwind.

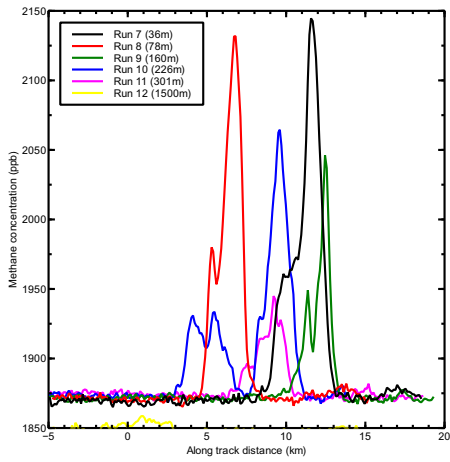


Figure 15: Raw methane measurements, flight B688, 15 nm downwind.

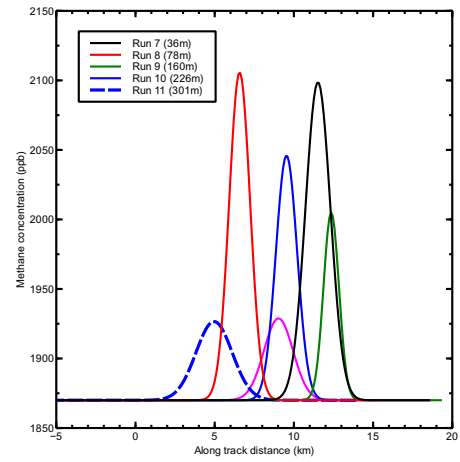


Figure 16: Fitted methane profiles, flight B688, 15 nm downwind.

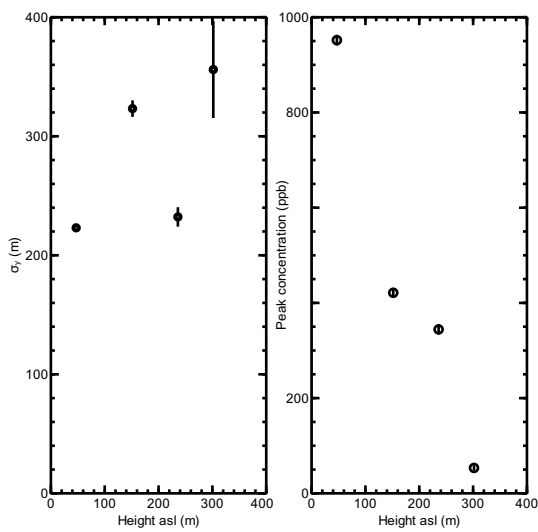


Figure 17: Variation of σ_y and C_z with height for plume measurements 5 nm downwind of the rig: flight B688.

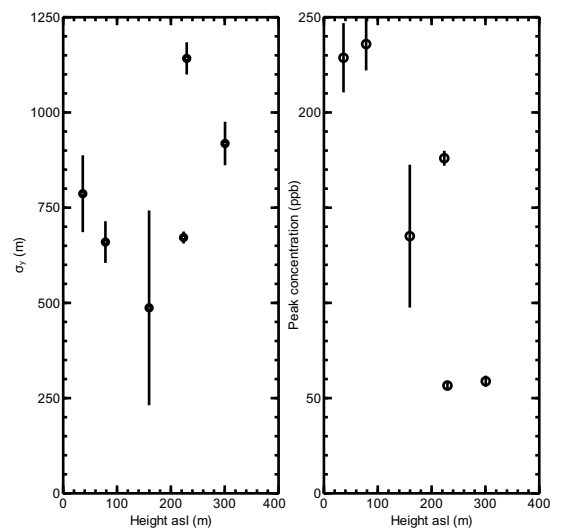


Figure 18: Variation of σ_y and C_z with height for plume measurements 15 nm downwind of the rig: flight B688.

5.2 Flight B689: 3 April 2012

5.2.1 Meteorology

The take-off time was 12:06 UTC. Figures (19) to (22) show the Met Office surface analysis chart and three satellite images for the period of the flight. A depression was centred just north of the Humber estuary at midday and was drifting slowly eastwards, with associated fronts over central UK and North Sea. The visible satellite images show unbroken cloud in the central North Sea with the Elgin rig towards the northern edge of the cloud. The infrared image shows that the cloud was deep. The wind around the Elgin region, to the north of the depression, was close to easterly throughout the flight. Although there were few breaks in the cloud layers, it did prove possible to locate sufficient breaks to descend to low levels. Once below the cloud, the aircraft remained at low levels until the measurements were complete, because of the risk of being unable to return to low level if unbroken cloud was penetrated.

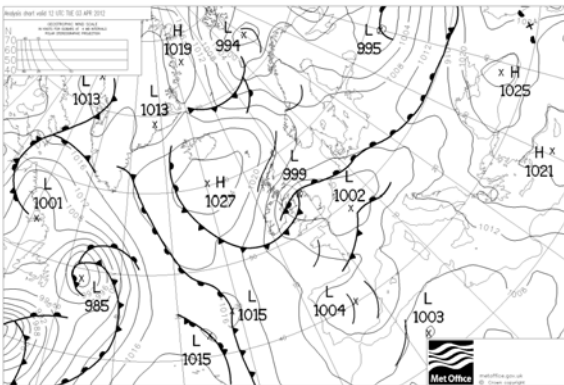


Figure 19: Surface analysis chart from the Met Office for 12:00 UTC on 3 April 2012.

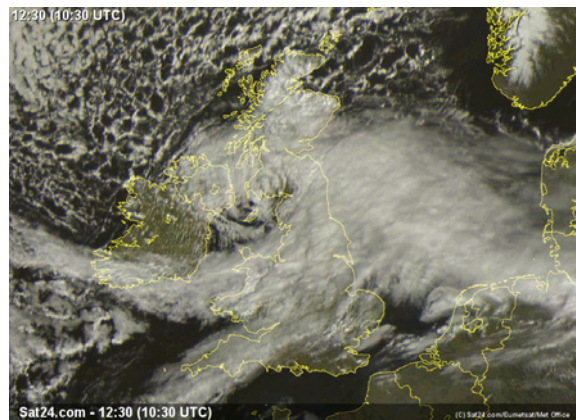


Figure 20: Meteosat visible satellite image for 10:30 UTC on 3 April 2012.

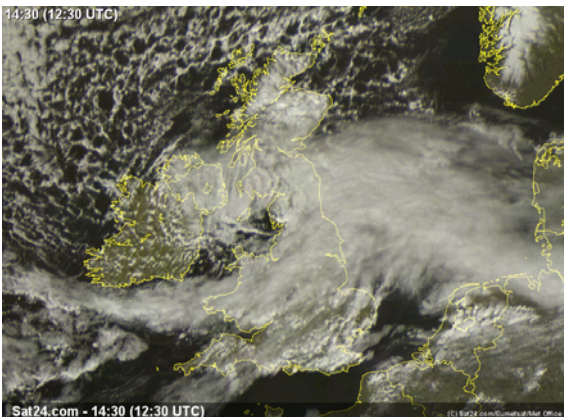


Figure 21: Meteosat visible satellite image for 12:30 UTC on 3 April 2012.

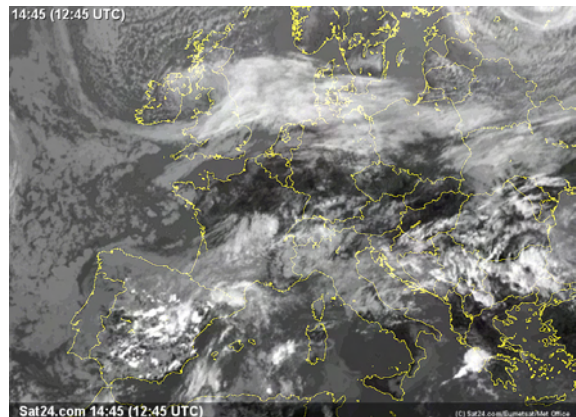


Figure 22: Meteosat infrared satellite image for 12:45 UTC on 3 April 2012.



Figure 23: Flight track for flight B689 on 3 April 2012. The position of the Elgin rig is marked in red.

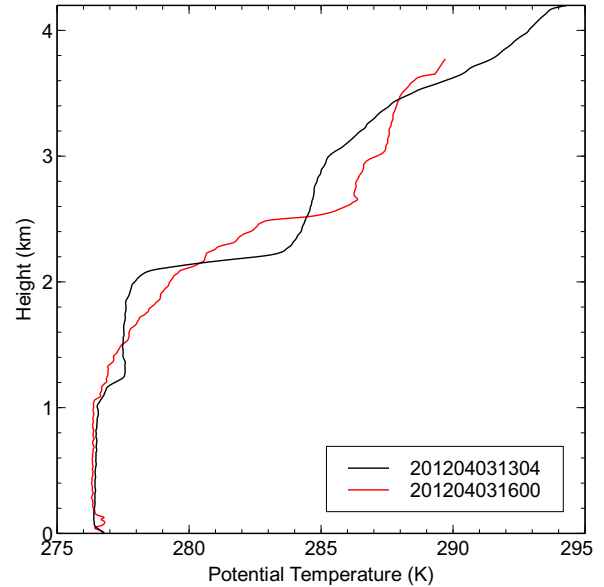


Figure 24: Atmospheric profiles from two dropsondes (launched early and late in the flight from locations close to Elgin) on 3 April 2012.

5.2.2 Measurements

The flight track is shown in Figure (23). Initially two passes were made across the line of the expected plume but around 5 nm upwind of the Elgin rig. These provided background methane concentrations. The aircraft was then repositioned downwind of the rig and repeated passes were made across the plume at two distances (approximately 5 nm and 15 nm) from the rig. Two long passes along the plume were made in order to collect air samples for later analysis. The procedure of making these collections during runs along the plume was adopted after the challenges of timing the collection to coincide with rapid passes across the plume became evident in flight B688. Mean wind speeds were around 12 ms^{-1} throughout.

Figures (25) and (26) show the measured and fitted (using the method described in §4.3) methane concentrations across the plume at approximately 5 nm downwind. Figure (31) shows the corresponding parameters σ_y and C_z from fitting the Gaussian plume equation (6) to this data. There is evidence for a decay of peak concentration with height at this distance downwind, consistent with the methane having not mixed through the full depth of the boundary-layer. Figure (24) shows potential temperature profiles from dropsondes launched at the start and end of the measurement part of the flight. There is good evidence of a stable layer/inversion just above 1 km altitude early in the flight. Below this there exists essentially neutrally stratified conditions. These conditions persisted throughout the flight, although as the later dropsonde profile shows, the stable layer above became weaker with time. The consistent decrease in plume concentration with height, coupled with the fact that the measurements were all made well below the inversion layer, suggests that the method 2 of §4.3 can be used.

Figures (27) and (28) show results for 15 nm downwind and Figures (29) and (30) show results for 25 nm downwind. Satisfactory Gaussian fits are evident in all cases. However Figures (32) and (33) show poor evidence of a decay of concentration with height. This lack of consistent decay, plus the clear existence of an inversion layer at just above 1 km, suggests that the assumption of mixing up to the inversion height may be made here. Method 1 was therefore used to calculate the methane flow rate from data at 15 nm and 25 nm from the rig, using a mixing height of $1.13 \pm 0.1 \text{ km}$. All flow rate results are shown in §5.7.

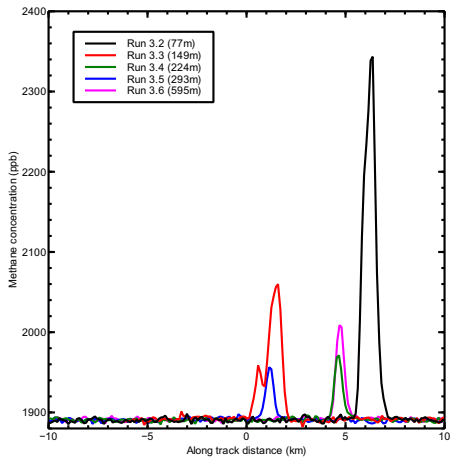


Figure 25: Raw methane measurements, flight B689, 5 nm downwind.

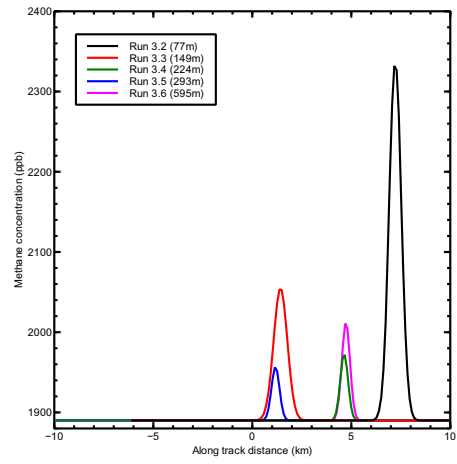


Figure 26: Fitted methane profiles, flight B689, 5 nm downwind.

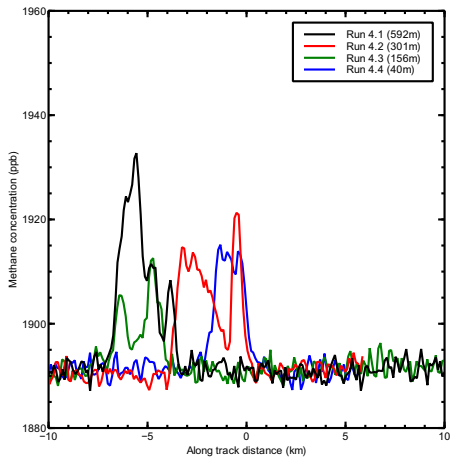


Figure 27: Raw methane measurements, flight B689, 15 nm downwind.

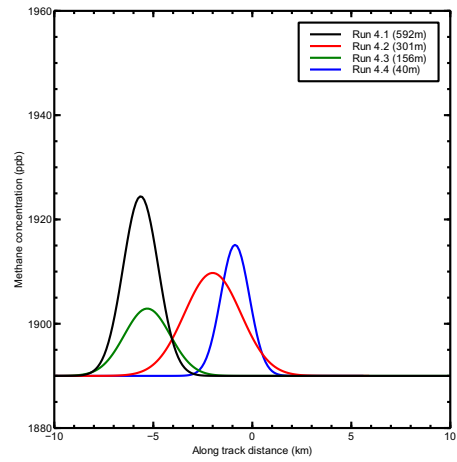


Figure 28: Fitted methane profiles, flight B689, 15 nm downwind.

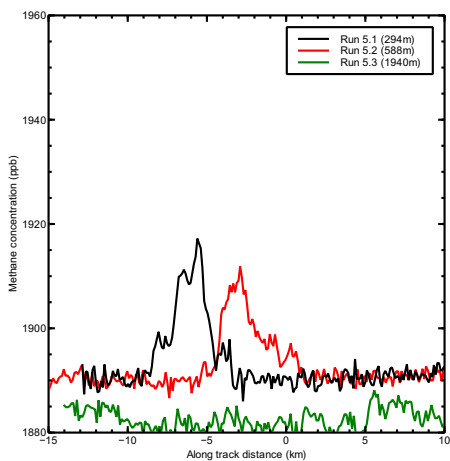


Figure 29: Raw methane measurements, flight B689, 25 nm downwind.

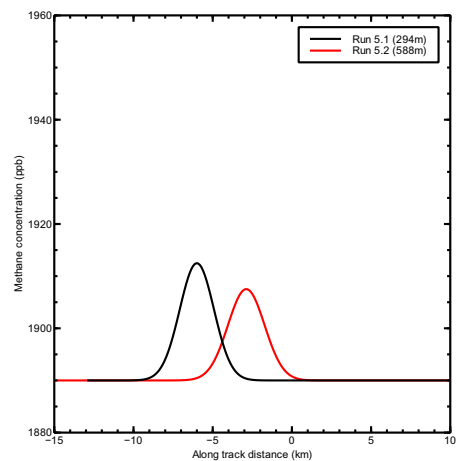


Figure 30: Fitted methane profiles, flight B689, 25 nm downwind.

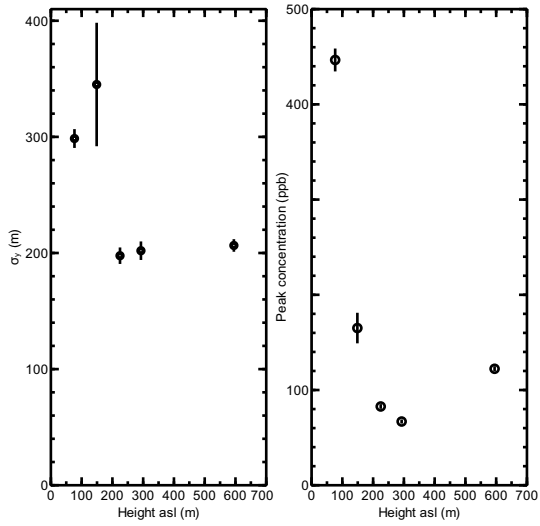


Figure 31: Variation of σ_y and C_z with height for plume measurements 5 nm downwind of the rig: flight B689.

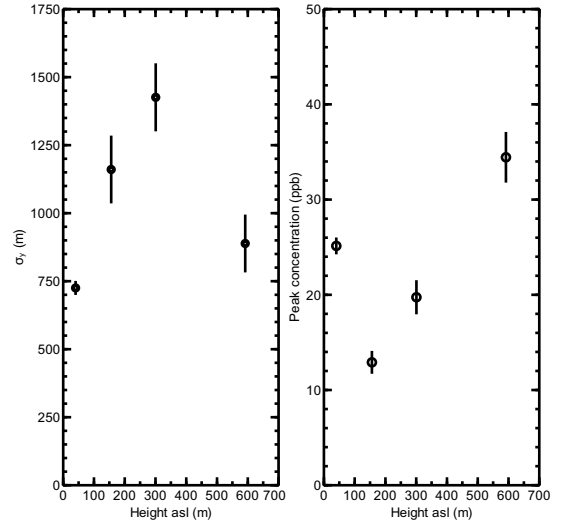


Figure 32: Variation of σ_y and C_z with height for plume measurements 15 nm downwind of the rig: flight B689.

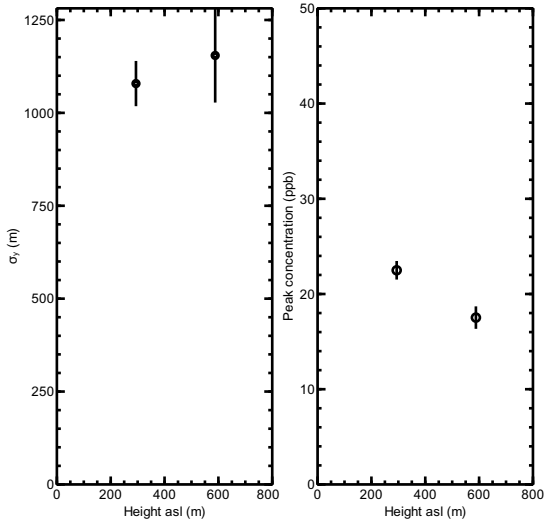


Figure 33: Variation of σ_y and C_z with height for plume measurements 25 nm downwind of the rig: flight B689.

5.3 Flight B690: 17 April 2012

5.3.1 Meteorology

The take-off time was 10:58 UTC. Figures (34) to (37) show the Met Office surface analysis chart and three satellite images for the period of the flight. A deep depression was centred west of Ireland with associated occluded fronts well ahead of the main low pressure centre over the North Sea. These fronts were moving quickly to the north east. The visible satellite images show the unbroken frontal cloud over and to the north east of the Elgin region. The flight take-off time was delayed to allow more time for the cloud to clear from the Elgin region during the operational period. This strategy was successful, allowing penetration through breaks in the cloud down to low levels. The infrared image shows that the cloud was deep but that the deepest cloud had already cleared the Elgin region. The wind around the Elgin region was south-south-easterly throughout the flight.

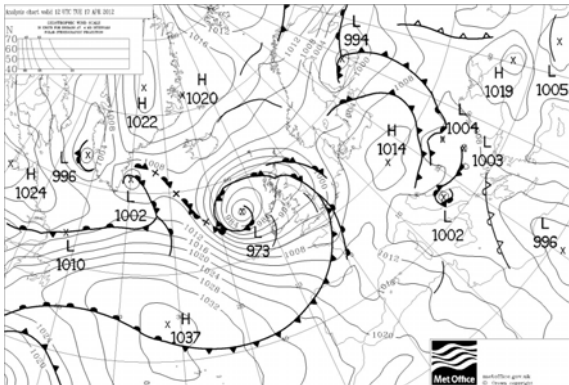


Figure 34: Surface analysis chart from the Met Office for 12:00 UTC on 17 April 2012.

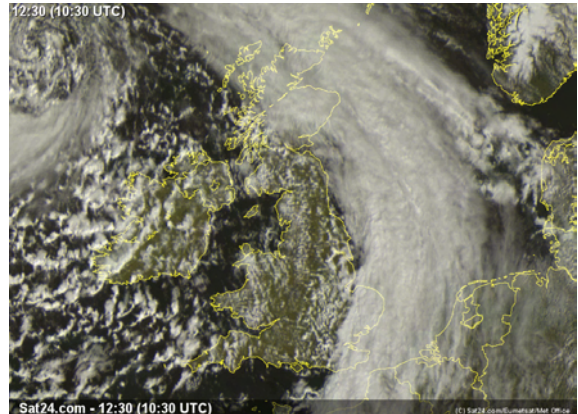


Figure 35: Meteosat visible satellite image for 10:30 UTC on 17 April 2012.

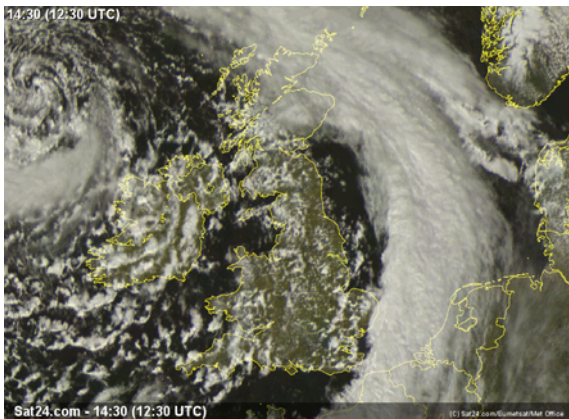


Figure 36: Meteosat visible satellite image for 12:30 UTC on 17 April 2012.

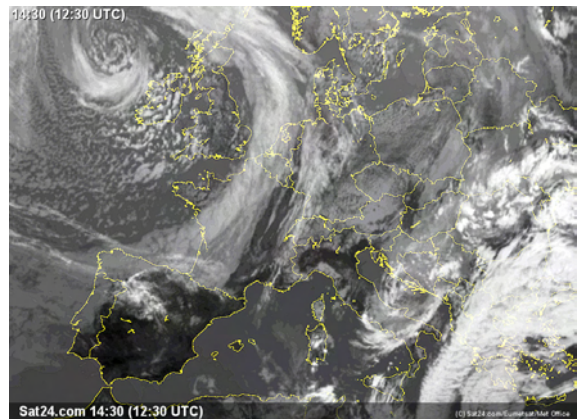


Figure 37: Meteosat infrared satellite image for 12:30 UTC on 17 April 2012.



Figure 38: Flight track for flight B690 on 17 April 2012. The position of the Elgin rig is marked in red.

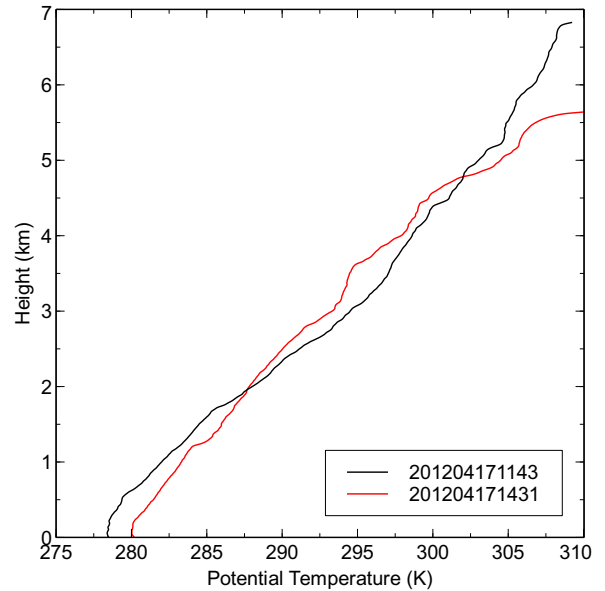


Figure 39: Atmospheric profiles from two dropsondes (launched early and late in the flight from locations close to Elgin) on 17 April 2012.

5.3.2 Measurements

The flight track is shown in Figure (38). Initially three passes were made across the line of the expected plume but around 5 nm upwind of the Elgin rig. These provided background methane concentrations. The aircraft was then repositioned downwind of the rig and repeated passes were made across the plume at two distances (approximately 5 nm and 20 nm) from the rig. Three diagonal passes were made across plume, following the procedure established in flight B689, in order to collect air samples for later analysis. Mean wind speeds were around 20 ms^{-1} throughout.

Figures (40) and (41) show the measured and fitted (using the method described in §4.3) methane concentrations across the plume at approximately 5 nm downwind. Figure (44) shows the corresponding parameters σ_y and C_z from fitting the Gaussian plume equation (6) to this data. Figures (42) and (43) show the measured and fitted methane profiles at 20 nm downwind and the fitted parameters σ_y and C_z are shown in Figure (45). There is evidence for a decay of peak concentration with height at both downwind distances, consistent with the methane having not mixed through the boundary-layer. Figure (39) shows potential temperature profiles from dropsondes launched at the start and end of the measurement part of the flight. The atmosphere appears to be stable at all levels above a very shallow (<200 m) mixed layer close to the surface. The rather uniform stability, coupled with the decay of concentration with height, supports the use of method 2 of §4.3 for calculating the methane flow rate.

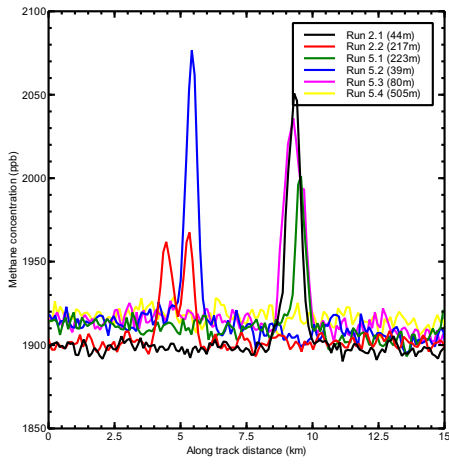


Figure 40: Raw methane measurements, flight B690, 5 nm downwind.

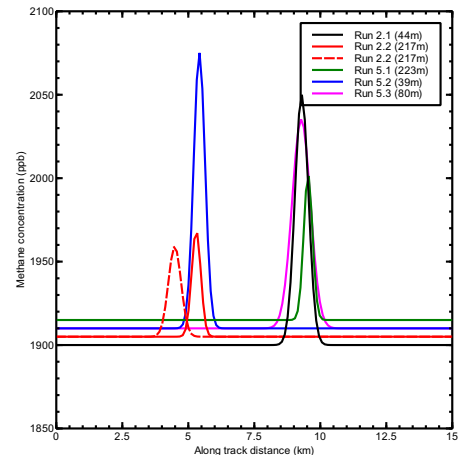


Figure 41: Fitted methane profiles, flight B690, 5 nm downwind.

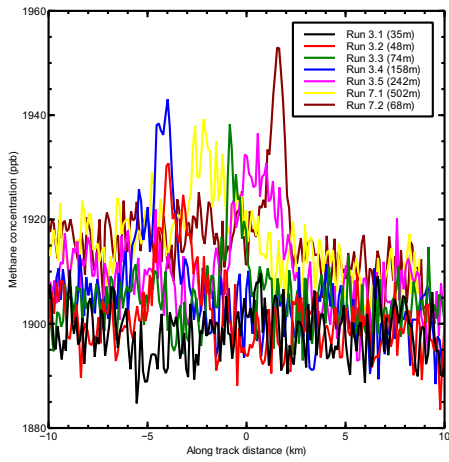


Figure 42: Raw methane measurements, flight B690, 20 nm downwind.

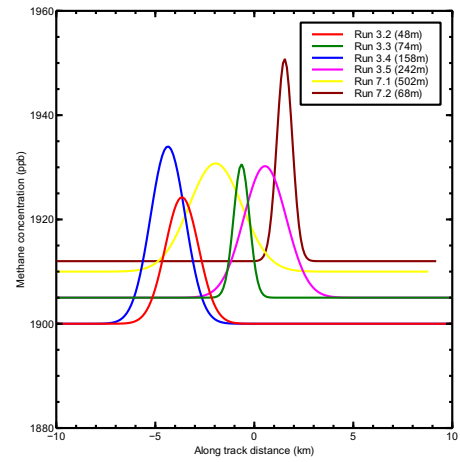


Figure 43: Fitted methane profiles, flight B690, 20 nm downwind.

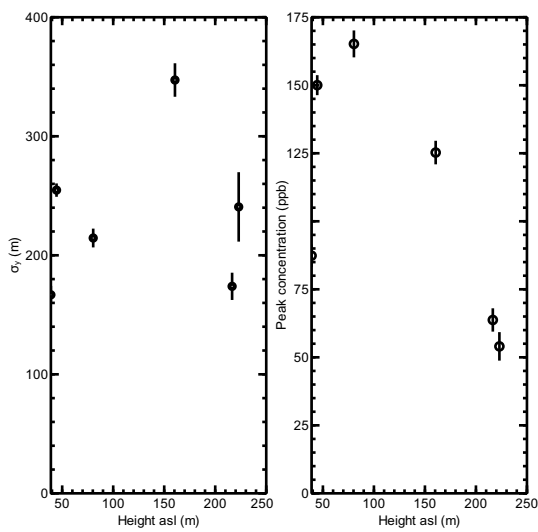


Figure 44: Variation of σ_y and C_z with height for plume measurements 5 nm downwind of the rig: flight B690.

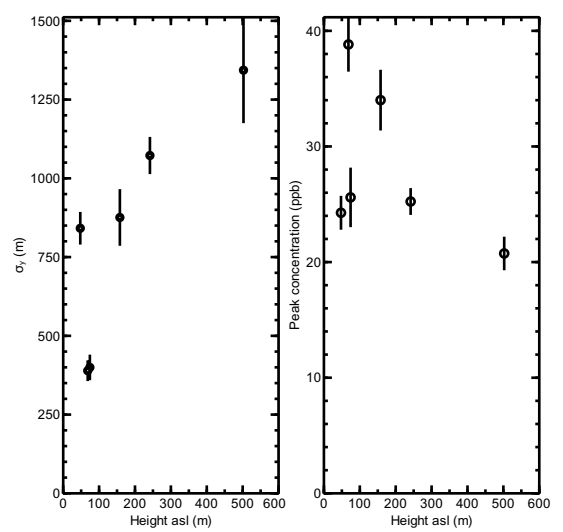


Figure 45: Variation of σ_y and C_z with height for plume measurements 20 nm downwind of the rig: flight B690.

5.4 Flight B691: 24 April 2012

5.4.1 Meteorology

The take-off time was 12:04 UTC. Figures (46) to (49) show the Met Office surface analysis chart and three satellite images for the period just before and during the flight. Over the North Sea there was a region of slack pressure gradient and light winds, with a tendency towards easterly. The visible satellite images show the broken cloud over the Elgin region. The infrared image shows only shallow cloud over the Elgin region. It was already clear before the flight that the light winds may be problematic on this day, with the possibility of poorly defined plumes.

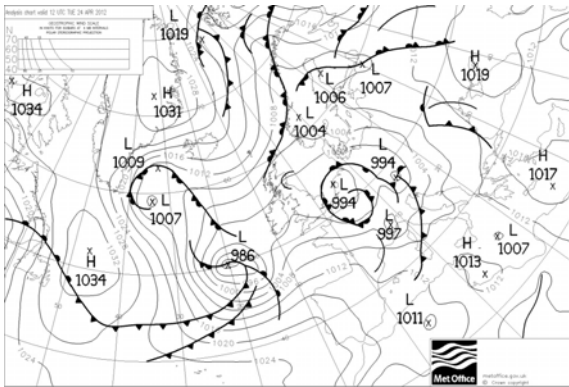


Figure 46: Surface analysis chart from the Met Office for 12:00 UTC on 24 April 2012.

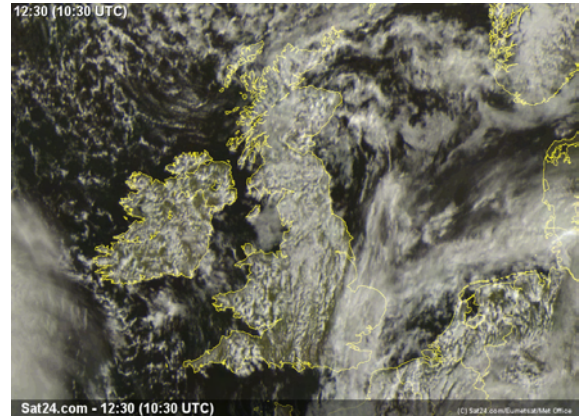


Figure 47: Meteosat visible satellite image for 10:30 UTC on 24 April 2012.

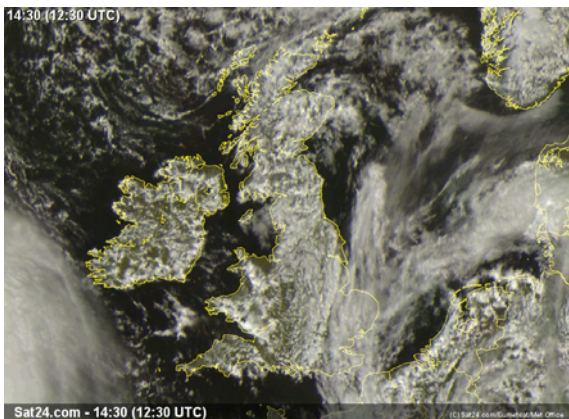


Figure 48: Meteosat visible satellite image for 12:30 UTC on 24 April 2012.

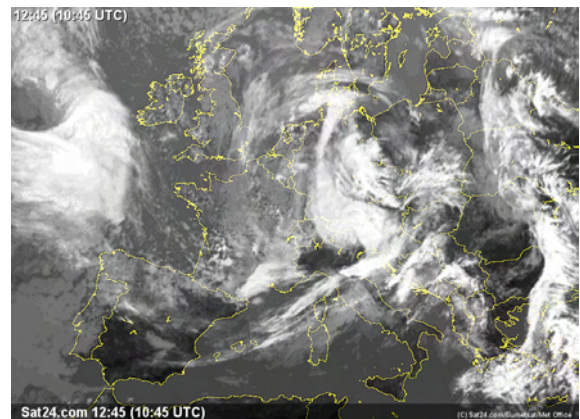


Figure 49: Meteosat infrared satellite image for 10:45 UTC on 24 April 2012.



Figure 50: Flight track for flight B691 on 24 April 2012. The position of the Elgin rig is marked in red.

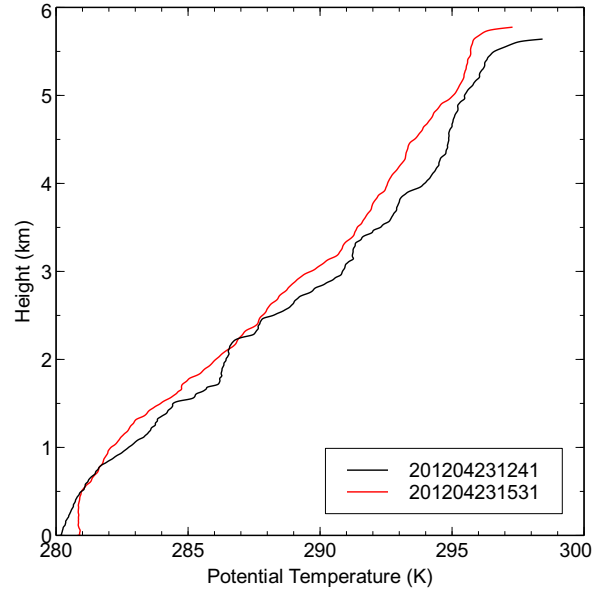


Figure 51: Atmospheric profiles from two dropsondes (launched early and late in the flight from locations close to Elgin) on 24 April 2012.

5.4.2 Measurements

The flight track is shown in Figure (50). Initially a pass was made across the line of the expected plume but approximately 5 nm upwind of the Elgin rig. This provided background methane concentrations. The aircraft was then repositioned downwind of the rig and repeated passes were made across the plume at two distances (approximately 5 nm and 20 nm) from the rig. Air samples were also collected on many of the transects through the plume for later analysis. Mean wind speeds were around 2-4 ms^{-1} from the east or north-east throughout.

Figures (52) and (53) show the measured and fitted (using the method described in §4.3) methane concentrations across the plume at approximately 5 nm downwind. Figure (56) shows the corresponding parameters σ_y and C_z from fitting the Gaussian plume equation (6) to this data. Figures (54) and (55) show the measured and fitted methane profiles at 20 nm downwind and the fitted parameters σ_y and C_z are shown in Figure (57). Figure (51) shows potential temperature profiles from dropsondes launched at the start and end of the measurement part of the flight. These show a generally stable atmosphere with some tendency to become mixed over the lowest 400 m later in the flight. There is no evidence of significant elevated inversions. At 5 nm downwind there is insufficient data for trustworthy conclusions to be drawn, particularly because even though there is little evidence of variation of concentration with height, there is no clear mixing height. There is evidence for a decay of peak concentration with height at 20 nm downwind, suggesting that method 2 may be applied here. It should be noted, however, that the plume transects at 5 nm show a rather ragged and broken plume and at 20 nm the plume is not well defined at all. The poor plume definition can be attributed to the low wind speed. Most of the transects have produced fitted Gaussian cross-sections but these cannot be considered to be of high reliability. So although the results at 20 nm have produced a methane flow rate using method 2, there is considerable uncertainty, due to the light winds, regarding whether all the methane plume filaments have been detected and the reliability of the overall result must be suspect. The principal conclusion from this flight is that stronger winds are required in order to reliably measure the flow rate.

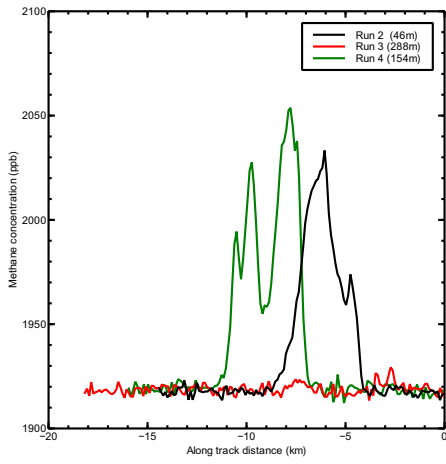


Figure 52: Raw methane measurements, flight B691, 5 nm downwind.

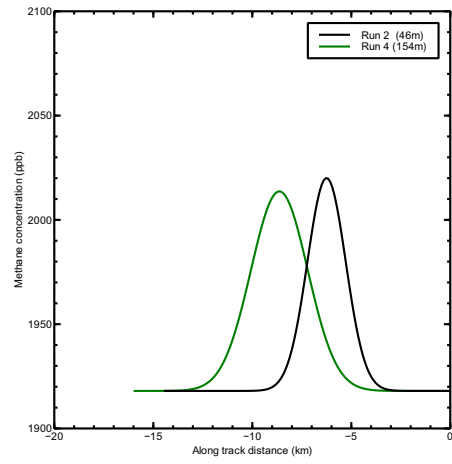


Figure 53: Fitted methane profiles, flight B691, 5 nm downwind.

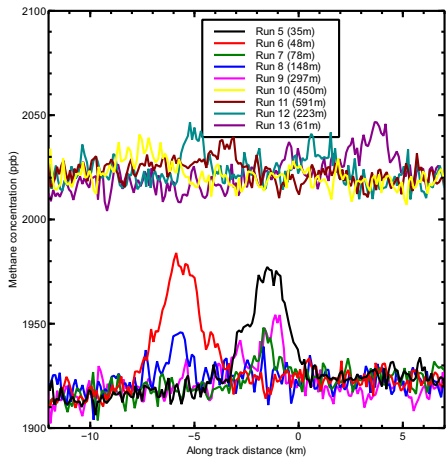


Figure 54: Raw methane measurements, flight B691, 20 nm downwind. Note that some data have been offset by adding 100 ppb for clarity of presentation.

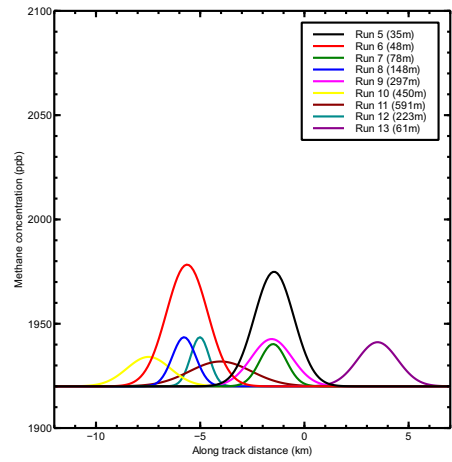


Figure 55: Fitted methane profiles, flight B691, 20 nm downwind.

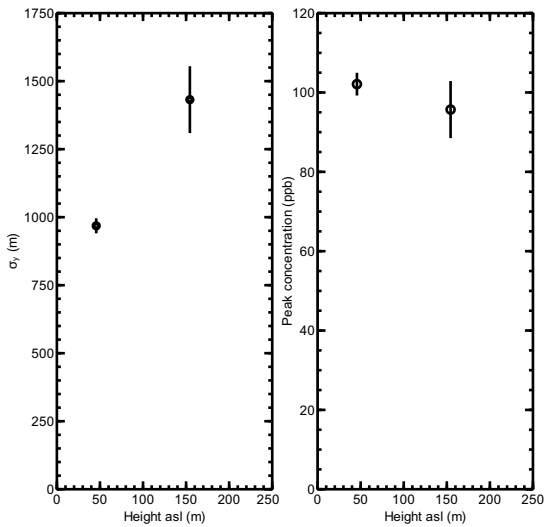


Figure 56: Variation of σ_y and C_z with height for plume measurements 5 nm downwind of the rig: flight B691.

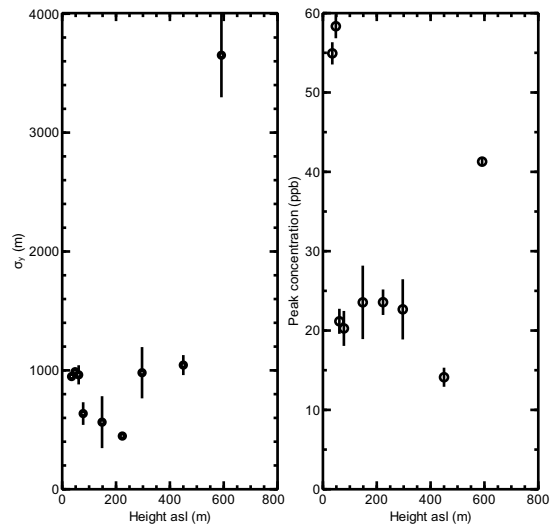


Figure 57: Variation of σ_y and C_z with height for plume measurements 20 nm downwind of the rig: flight B691.

5.5 Flight B693: 4 May 2012

5.5.1 Meteorology

The take-off time was 12:32 UTC. Figures (58) to (61) show the Met Office surface analysis chart and three satellite images for the period before and during the flight. An anticyclone was centred between Scotland and Iceland with a depression centred over southern Scandinavia. Between these two weather systems was a showery northerly flow. The visible satellite images show showers, with some organisation into bands in places. The infrared image nevertheless shows that the shower activity was quite shallow. Breaks in the cloud were sufficient to allow penetration of the aircraft to low levels, below cloud base. The wind speed around the Elgin region was 10-20 ms⁻¹ and from a northerly or north-easterly direction.

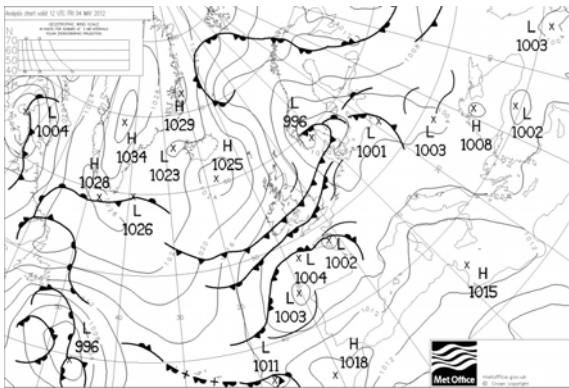


Figure 58: Surface analysis chart from the Met Office for 12:00 UTC on 4 May 2012.

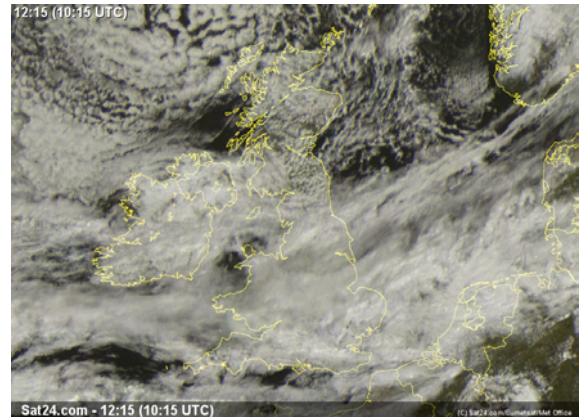


Figure 59: Meteosat visible satellite image for 10:15 UTC on 4 May 2012.

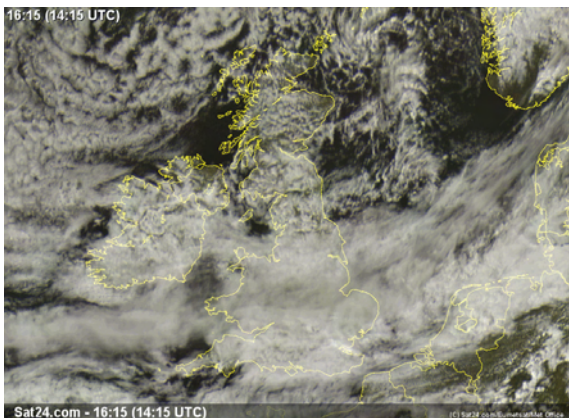


Figure 60: Meteosat visible satellite image for 14:15 UTC on 4 May 2012.

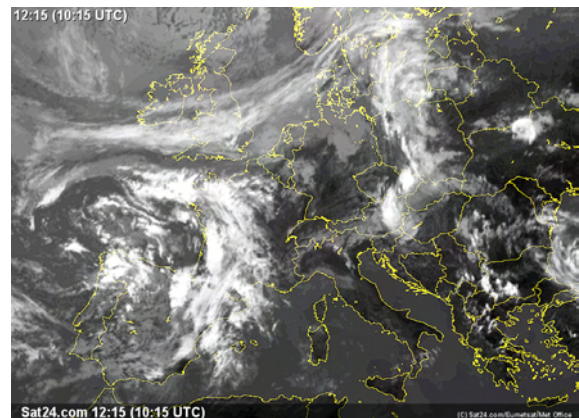


Figure 61: Meteosat infrared satellite image for 10:15 UTC on 4 May 2012.



Figure 62: Flight track for flight B693 on 4 May 2012. The position of the Elgin rig is marked in red.

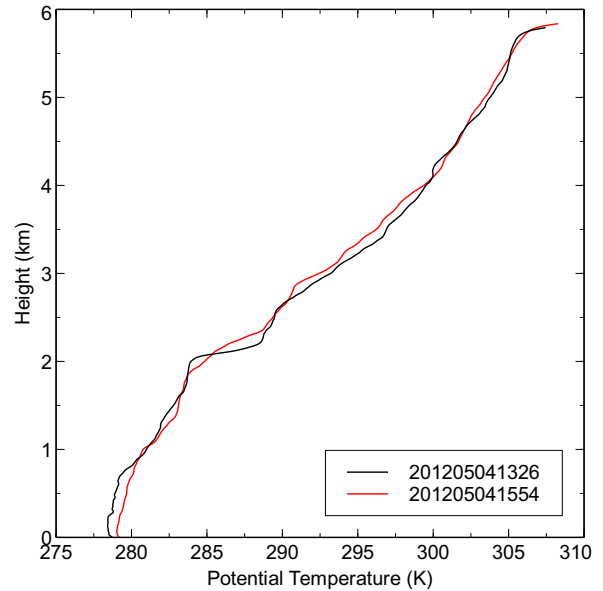


Figure 63: Atmospheric profiles from two dropsondes (launched early and late in the flight from locations close to Elgin) on 4 May 2012.

5.5.2 Measurements

The flight track is shown in Figure (62). Initially two passes were made across the line of the expected plume but around 5 nm upwind of the Elgin rig. These provided background methane concentrations. The aircraft was then repositioned downwind of the rig and repeated passes were made across the plume at two distances (approximately 5 nm and 20 nm) from the rig. A single pass along the plume was made in order to collect air samples, along with additional air samples collected during the transects across the plume. Mean wind speeds were around $10\text{-}20\text{ ms}^{-1}$ throughout.

Figures (64) and (65) show the measured and fitted (using the method described in §5.7) methane concentrations across the plume at approximately 5 nm downwind. Figure (68) shows the corresponding parameters σ_y and C_z from fitting the Gaussian plume equation (6) to this data. Figures (66) and (67) show the measured and fitted methane profiles at 20 nm downwind and the fitted parameters σ_y and C_z are shown in Figure (69). There is evidence for a decay of peak concentration with height at both downwind distances, consistent with the methane having not mixed through the boundary-layer. Figure (63) shows potential temperature profiles from dropsondes launched at the start and end of the measurement part of the flight. The atmosphere appears to be generally stable at all levels above a shallow (<300 m) mixed layer close to the surface. There is evidence of a significant inversion above 2 km at the start of the flight but no inversion at lower levels. The data show that the methane has definitely not mixed up to 2 km. The rather uniform stability at lower levels, coupled with the decay of concentration with height, supports the use of method 2 of §4.3 for calculating the methane flow rate.

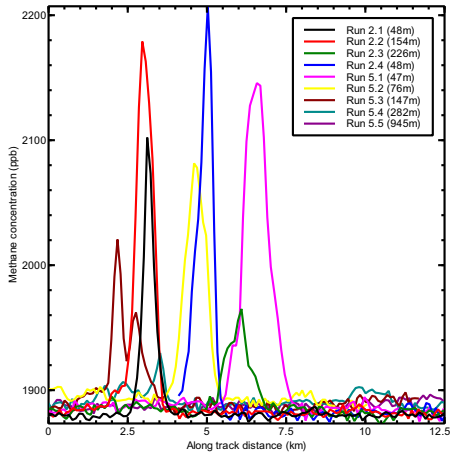


Figure 64: Raw methane measurements, flight B693, 5 nm downwind.

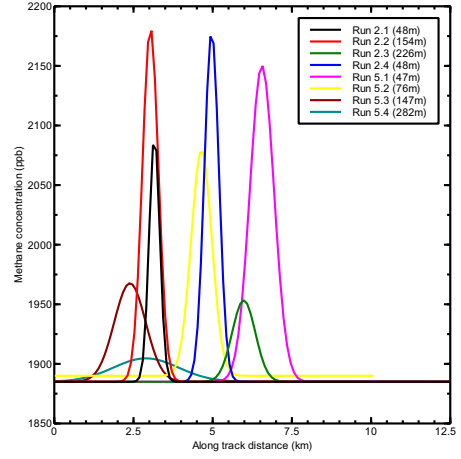


Figure 65: Fitted methane profiles, flight B693, 5 nm downwind.

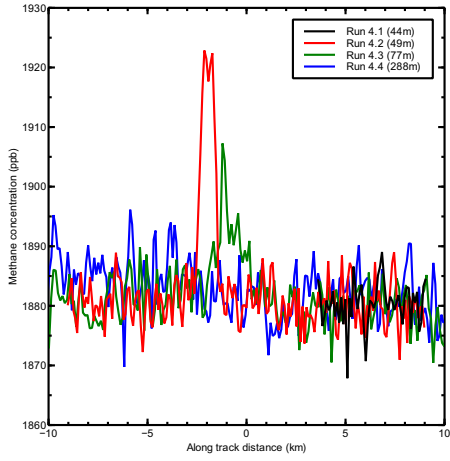


Figure 66: Raw methane measurements, flight B693, 20 nm downwind.

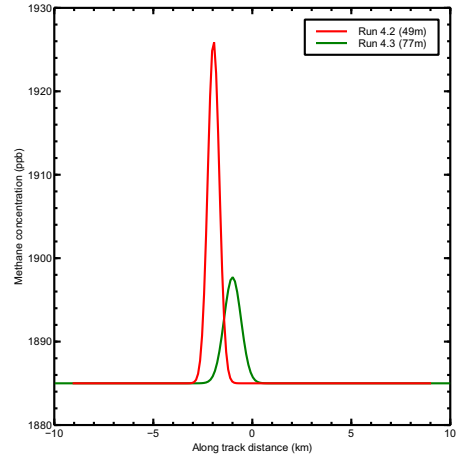


Figure 67: Fitted methane profiles, flight B693, 20 nm downwind.

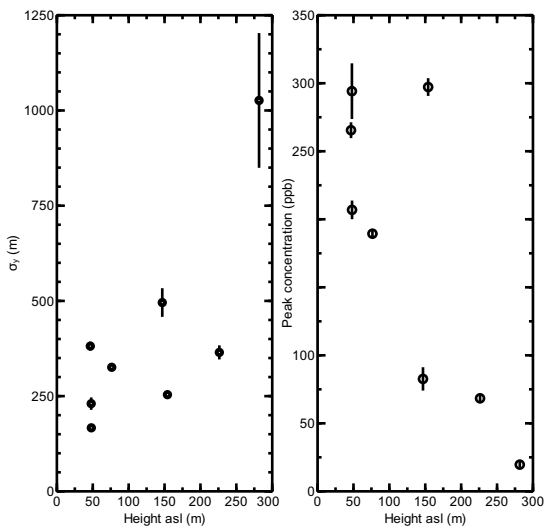


Figure 68: Variation of σ_y and C_z with height for plume measurements 5 nm downwind of the rig: flight B693.

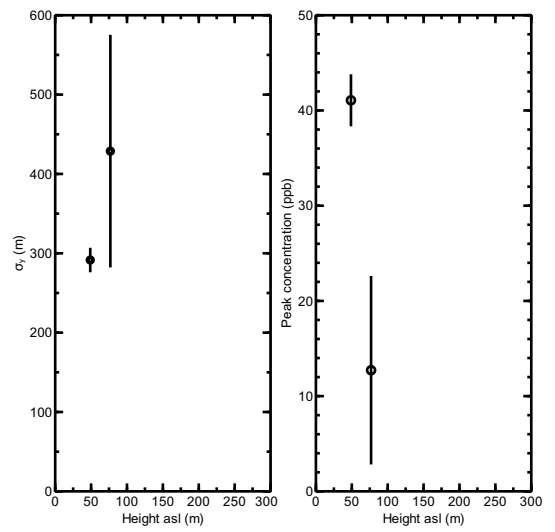


Figure 69: Variation of σ_y and C_z with height for plume measurements 20 nm downwind of the rig: flight B693.

5.6 Flight B727: 15 August 2012

5.6.1 Meteorology

The take-off time was 07:46 UTC. Figures (70) to (73) show the Met Office surface analysis chart and three satellite images for the period of the flight. A deep depression was centred south-west of Ireland with a slack pressure region over Scandinavia. Between these there was a south-easterly flow over the North Sea. The visible satellite images show low cloud over the western North Sea, gradually clearing during the flight. From the infrared image it is clear that the frontal cloud from the intense depression was still distant from Elgin. Breaks in the cloud were sufficient to allow penetration of the aircraft to low levels, below cloud base. The wind speed around the Elgin region was $8\text{-}15\text{ ms}^{-1}$ and from a south-easterly direction.

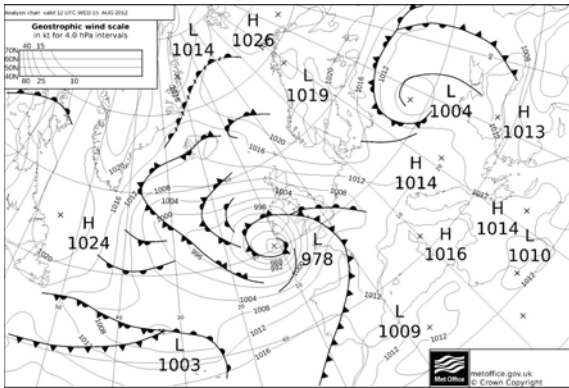


Figure 70: Surface analysis chart from the Met Office for 12:00 UTC on 15 August 2012.

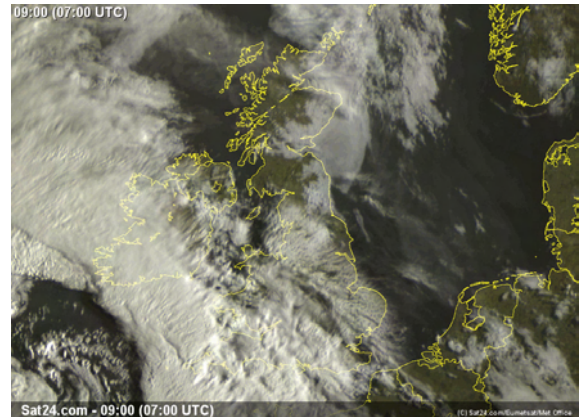


Figure 71: Meteosat visible satellite image for 07:00 UTC on 15 August 2012.

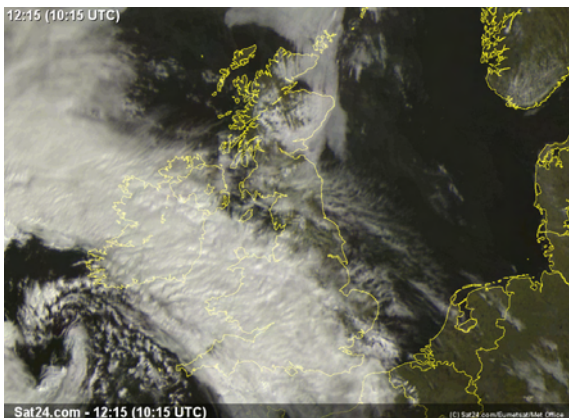


Figure 72: Meteosat visible satellite image for 10:15 UTC on 15 August 2012.

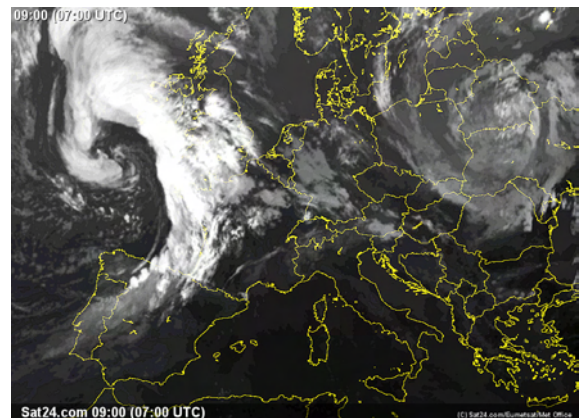


Figure 73: Meteosat infrared satellite image for 07:00 UTC on 15 August 2012.

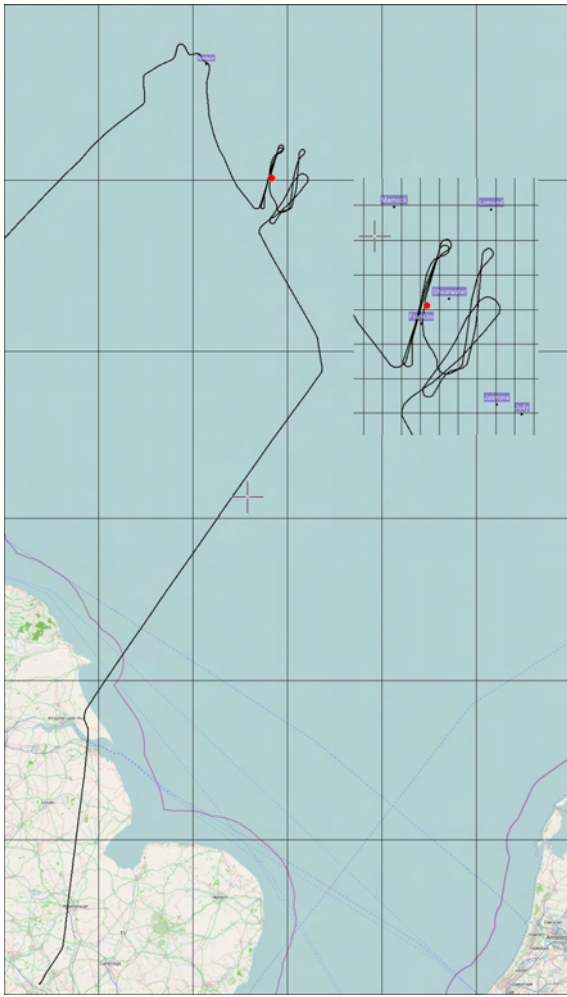


Figure 74: Flight track for flight B727 on 15 August 2012. The position of the Elgin rig is marked in red. Other rigs are also marked.

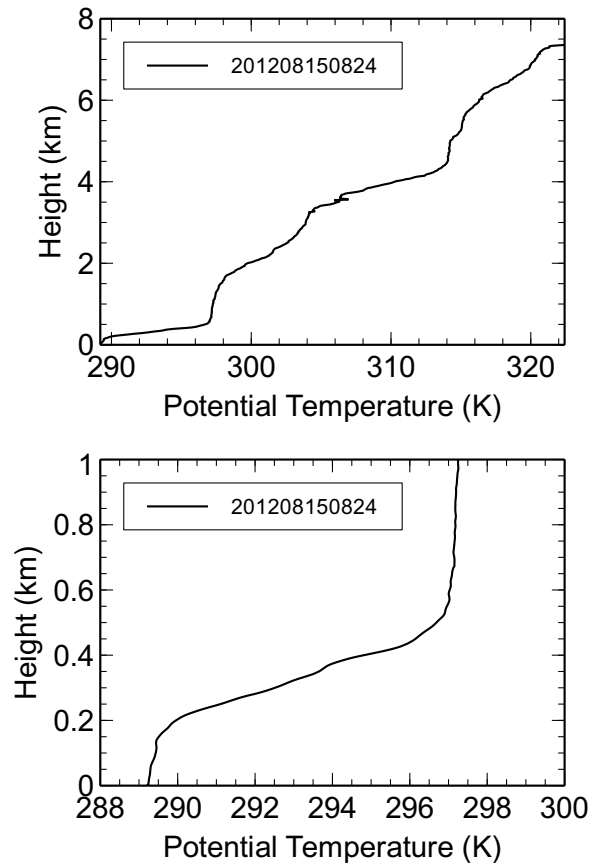


Figure 75: Atmospheric profiles from a dropsonde (launched from a location close to Elgin) on 15 August 2012.

5.6.2 Measurements

The objectives of this flight were:

- (a) to confirm that the methane leak from Elgin had been effectively capped and
- (b) to gain further information concerning background sources of trace gases from oil and gas installations, in order to assist with interpretation of previous (and potential future) research flights.

In support of these two aims, flight legs were made across the expected line of any plume from the Elgin rig, as in previous flights (these were made closer to Elgin than in previous flights as the air exclusion zone previously operating within 3 nm of the rig had been lifted). The flight track is shown in Figure (74).

The primary result from this flight was that there was no detectable methane plume from the Elgin rig.

The potential temperature from a single dropsonde launched from close to the Elgin rig during this flight is shown in Figure (75). The profile is quite unlike previous ones, with a shallow well-mixed layer up to approximately 200 m, above which was a stable layer up to approximately 500 m. This would indicate the potential for pollutant trapping below 200 m. Above 500 m the atmosphere was again well mixed. Transects were made below 200 m, between 200 and 500 m and above 500 m. In no case was a methane signal detected, in contrast to all previous flights.

5.7 Methane Flow Rate Results and Discussion

The methane flow rates calculate from the plume measurements and analysis from flights B688, B689, B690, B691 and B693 are summarised in Figure (76). Error bars have been deduced from the analysis detailed in §4.3.3. The results indicate:

- (a) There was a significant decrease in methane flow rate between 30 March and 4 April 2012.
- (b) There was no further detectable decrease in flow rate up to and including 4 May 2012.
- (c) The results from the flight on 24 April 2012 (B691) are not considered trustworthy due to the extreme low wind speeds. The possibility that parts of the plume were missed due to irregular dispersion cannot be ruled and is consistent with the apparent observation that the deduced flow rate on this day was lower than any previous or subsequent day.
- (d) When applicable, both methods 1 and 2 described in §4.3 give reliable and consistent flow rate estimates.

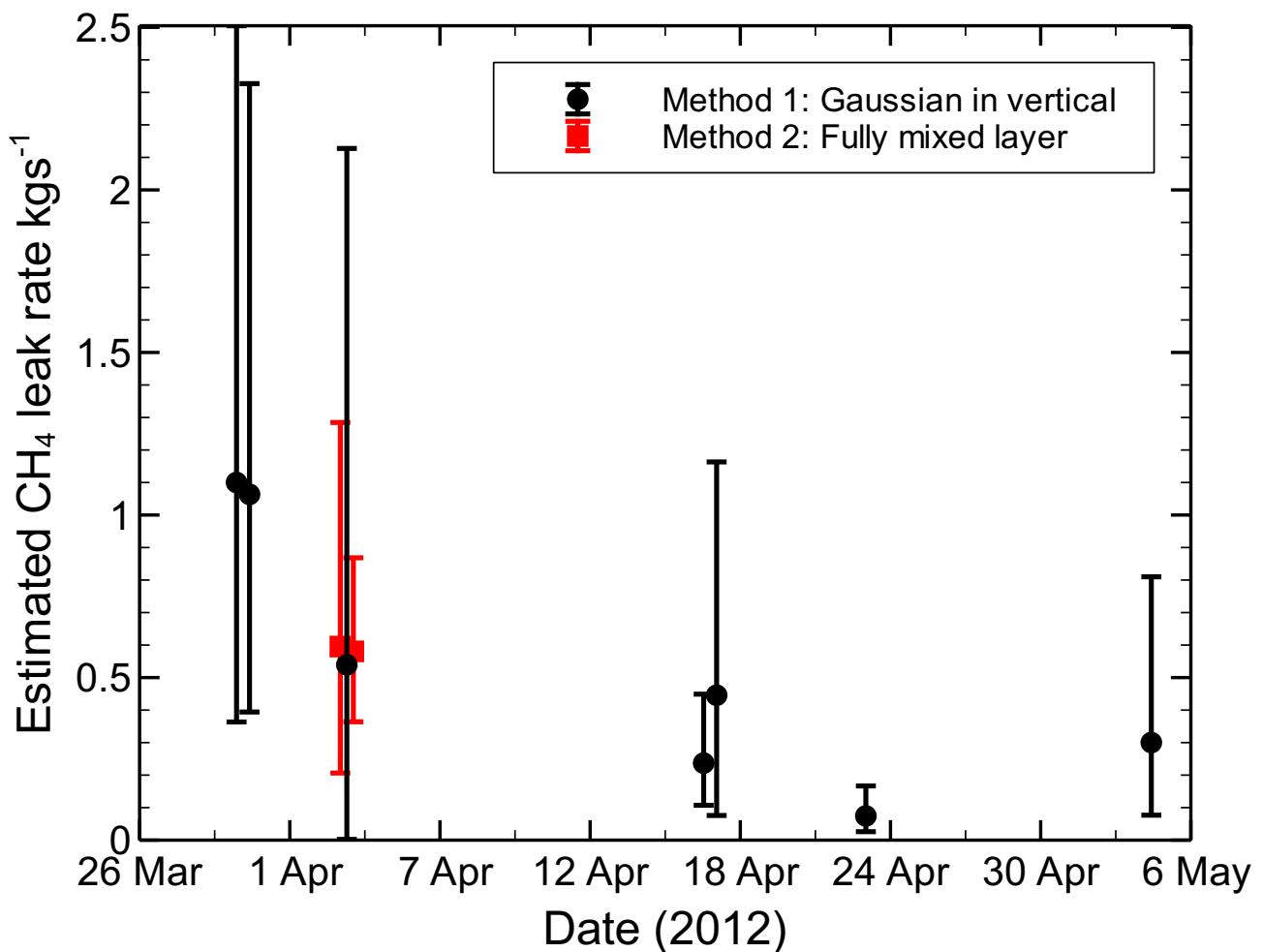


Figure 76: Methane flow rate from flights B688, B689, B690, B691 and B693. The symbols in black show flow rates calculated using method 2 and those in red show flow rates calculated using method 1. Multiple results from the same flight are from different distances downwind from the Elgin rig and/or from different calculation methods. The time separation of multiple results from the same flight have been slightly exaggerated for clarity.

It is noteworthy that on only one flight was it possible to use the fully mixed boundary-layer assumption (method 1 of §4.3). This contrasts with the experience of the Deepwater Horizon incident reported by Ryerson et al. (2011). There are several possible factors contributing to this:

1. For the majority of the flights there was no clear capping inversion to the boundary-layer.
2. The plume source was buoyant due to burning in the Deepwater Horizon event whereas for the Elgin leak, buoyancy is likely to have been much less significant. Although the gas temperature from the HOD

formation where the gas is thought to have originated is $\sim 165^{\circ}\text{C}$, considerable cooling is likely to have occurred before the gas reached the sea surface.

3. The lower concentrations of gases from the Elgin leak required measurements to be made closer to the source than during the Deepwater Horizon incident, allowing less time for vertical mixing.
4. The sea surface temperatures and near-surface air temperatures were similar in all cases for the Elgin flights. This indicates only small air-sea heat fluxes and low tendency for buoyant generation of turbulence. All of the flights during the period of the leak indicate small sea to air heat fluxes, with this being reversed for the single August flight.

In support of point (4) above, the sea surface temperature for the period of the flights is given in Figures (77) and (78), along with the near-surface air temperature. The sea surface temperature is from the NOAA Comprehensive Large Array-Data Stewardship System (<http://www.class.ngdc.noaa.gov/saa/products/welcome> (2012)). The air temperatures are from the Ekofisk radiosounding on 30 March and on other dates from the dropsondes released by the FAAM aircraft.

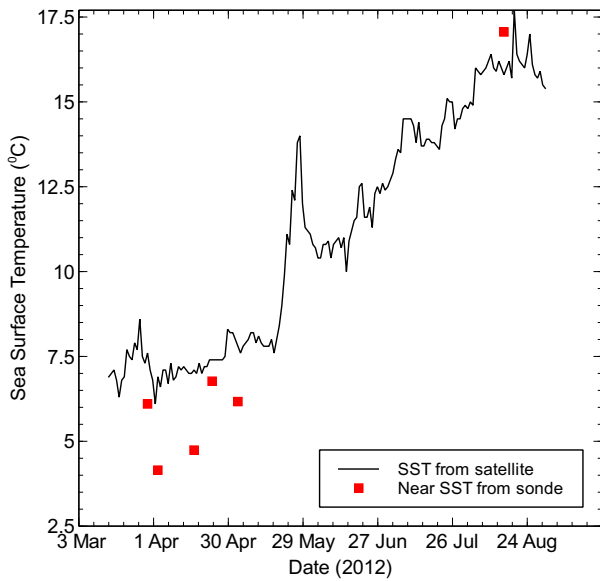


Figure 77: NOAA 100 km global Sea Surface Temperature (data-set derived from 8 km resolution satellite images). Air temperatures from radiosoundings and dropsondes.

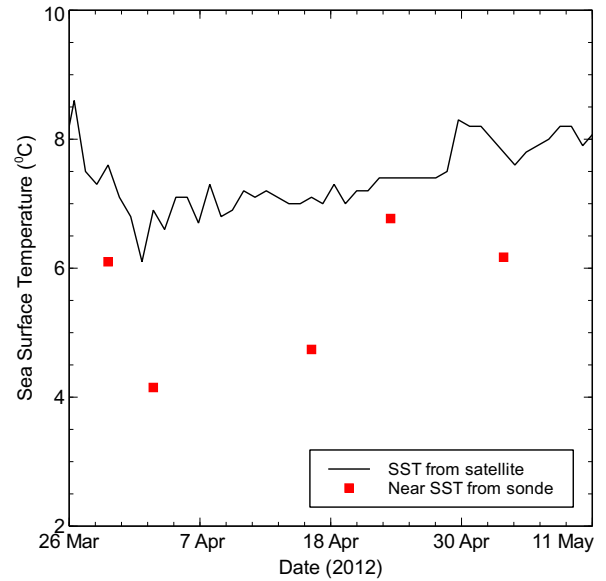


Figure 78: NOAA 100 km global Sea Surface Temperature (data-set derived from 8 km resolution satellite images). Air temperatures from radiosoundings and dropsondes.

5.8 Analysis of Non-methane Hydrocarbon and Other Organic Emissions

5.8.1 Results

Non-methane hydrocarbons and other volatile organic compounds in the Elgin plumes were determined from around 150 WAS samples. Around 20 distinct in-plume samples were collected, plus a further 10 with evidence of some plume contribution. The remaining samples were indicative of background hydrocarbons over the North Sea. Samples were referenced to the in-flight measurements of CH₄ and also for some flights to further detailed analysis of CH₄ and carbon isotopes made from air within the canisters themselves. Within the Elgin gas plume NMHC content was dominated by light alkanes (Table 1) with species ranging from >20 ppb ethane to <1 ppb benzene and <0.1 ppb higher monoaromatics.

Table 1: NMHC results for Elgin flights B688 to B693

Species	Average composition % Mol.	TOTAL ² estimate % Mol.	Highest in-plume WAS sample in ppb	Typical background in ppb
Methane	83.7	73	2010	~1850
Ethane	6.9	8.3	24.9	~2
Propane	3.5	3.9	12.72	~0.4
Iso-butane	0.8	0.8	2.95	<0.1
n-butane	1.4	1.5	5.14	<0.2
Iso-pentane	0.8	0.6	3.39	<0.1
n-pentane	0.8	0.8	2.44	<0.1
2,3-methyl-pentane	0.6		1.1	<0.05
Hexane	0.5	1.7 ³	1.54	<0.05
Benzene	0.1		0.47	<0.1
Heptane	0.4		1.44	<0.05
Toluene	0.4		1.42	<0.05
Ethyl benzene	0.02		0.08	<0.02
M+p xylene	0.3		0.76	<0.02
Oxylene	0.03		0.1	<0.02
Sum other higher HC (to nC14)	2.1	9.6	~4	<0.5

A close relationship between CH₄ and NMHCs was observed in plume samples with consistent proportionation – see Figure 79. The plume was dominated by linear and branched chain alkanes and some monoaromatic compounds, up to C5 alkylation. The presence of very elevated ethane and propane within the plumes was highly indicative of an above sea-surface emissions source. The light alkane species are sub-saturated in sea-water and are generally removed to the water column if released at the seabed; only the less soluble higher hydrocarbons reach the atmosphere. This was the case with the Deepwater Horizon accident where only the higher HCs were observed with aircraft sampling. Figure 80 shows the higher hydrocarbons detected using the GCxGC analysis. No polycyclic aromatic compounds or oxygenated species were observed. The spatial mixing of higher condensate species with background air was closely related to CH₄ and the C2-C4 NMHCs, indicating that emission to atmosphere was from the point-source leak. Atmospheric measurements showed a lower proportion of +C6 species than reported in Isaksen (2004) for Elgin reservoir fluids (~4% vs 13%), which may be rationalized by considering these larger species condensing as liquids to the sea surface rather than transport in the gas phase. The distribution of C1 to C2 – C4 species was generally in line with Isaksen estimates (data available only in graphical format, so cannot be tabulated) and also with those estimates provided by TOTAL (via email). The NMHC data from the FAAM showed no evidence for widespread higher condensate evaporation (e.g. larger >C6 hydrocarbons) into air from the seawater sheen. This would suggest condensate removal was by biological processes in the water.

²Re-normalised to remove CO₂/N₂ contributions since these not assessed in FAAM plume flights.

³Unclear whether this value is for the n-hexane isomer alone or all C6. If the latter then the observations are in better agreement with TOTAL estimate.

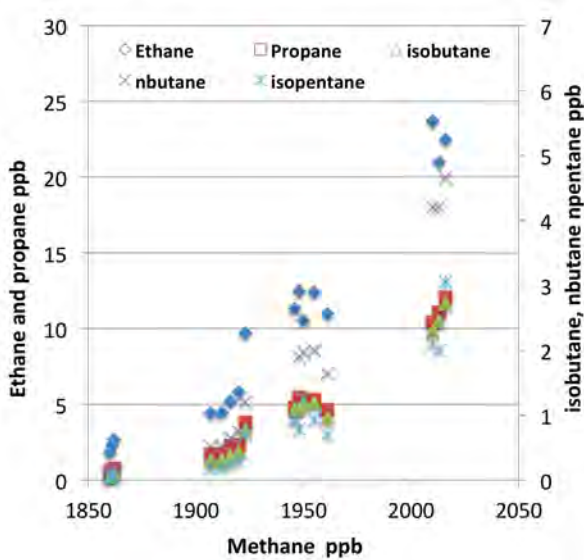


Figure 79: NMHC relationships to CH_4 within the Elgin platform plumes.

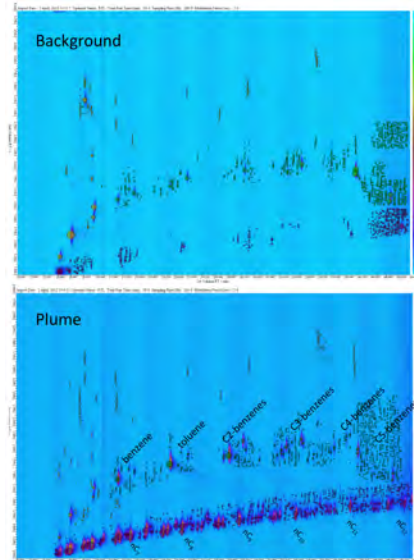


Figure 80: Plume (lower) and background (upper) GCxGC chromatograms with analysis of alkanes and aromatic species in range nC5-nC12.

If the NMHC concentrations for individual flights are examined, the overall trend appears to be an increasing fractional NMHC content with time, although with no significant change in the overall NMHC distribution, which is overwhelmingly paraffinic. Aromatic content remained low throughout. Table (2) and Figures (81) and (82) show the evolution of NMHC concentrations with time. The data are consistent with the hypothesis that the lighter methane from the leaking formation preferentially escaped before the heavier NMHCs.

% Mol.	B688	B689	B690	B691	B693
Methane	81.0	86.5	79.0	73.4	69.7
Ethane	7.9	5.9	8.8	11.3	13.1
Propane	4.3	2.7	4.0	5.4	6.1
iso-butane	1.0	0.6	0.9	1.2	1.4
n-butane	1.7	1.0	1.4	1.98	2.2
iso-pentane	1.1	0.4	0.8	1.08	1.2
n-pentane	0.8	0.7	0.8	1.03	1.2
2,3-methyl-pentane	0.5	0.6	0.5	0.71	0.8
Hexane	0.6	0.4	0.5	0.68	0.8
Benzene	0.1	0.1	0.1	0.16	0.2
n-heptane					0.39
Toluene					0.4
Ethyl benzene					0.02
m+p xylene					0.3
Oxylene					0.01
Other higher HC (best estimate)	1.0	1.2	3.1	3.1	2.2

Table 2: NMHC concentrations for each flight.

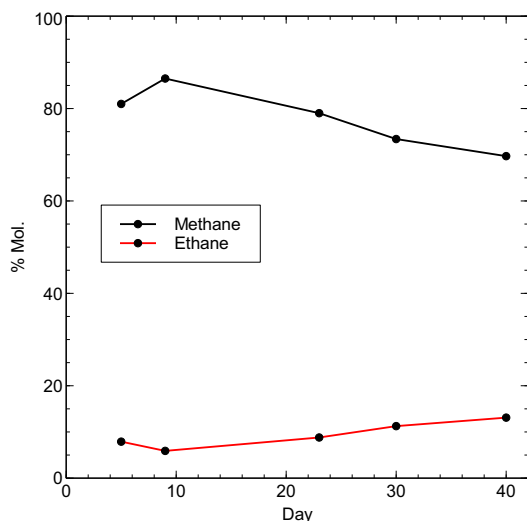


Figure 81: Evolution of methane and ethane concentrations with day number (from 26 March).

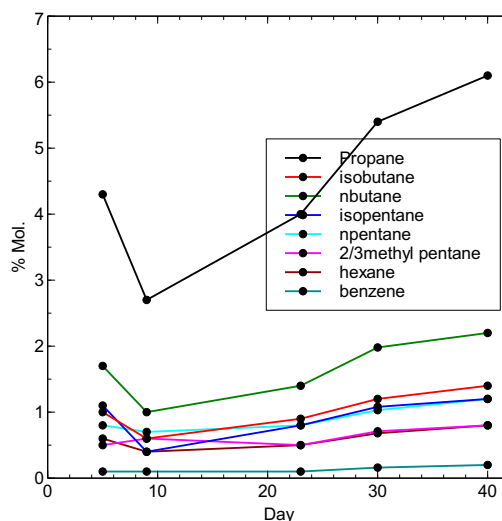


Figure 82: Evolution of NMHC concentrations with day number (from 26 March).

5.8.2 Atmospheric Chemistry impacts

The paraffinic nature of the Elgin emissions, and the limited emission of reactive monoaromatic compounds, resulted in a relatively unreactive ensemble of hydrocarbons. In the absence of any substantial co-located NO_x releases, as would be expected, the aircraft did not observe detectable ozone formation downwind of the platform. The size and scale of the leak did however provide some perturbation to the regional background in light alkanes, which in time would likely feed through in to a very small tropospheric ozone increase. A perturbation in background propane/butane ratios was reported at the Jungfraujoch observatory in the Swiss alps and the Rigi observatory in Latvia more than 1000 km downwind (EMPA, Switzerland, Reiman S., personal communication). It appears likely that following further analysis a number of other background stations may well also report detection of the Elgin plume far downwind of source. Some initial discussion of these findings is given in §4.4.1 but more definite conclusions would require both further analysis of observations and further modelling using a chemical transport model. Note that events such as these are of particular academic interest to atmospheric scientists since they provide this opportunity to test model performance, rather than any direct environmental impact.

6 Summary & Recommendations

6.1 Summary of Results

6.1.1 Flow rate

All five flights between 30 March and 4 May provided estimates of methane flow rate. One flight (3 April) generated data which could be analysed for total flow rate using the assumption of a well-mixed boundary-layer, with cross-plume structure being approximated by a fitted Gaussian profile (method 1). For this flight flow rate estimates were also obtained by fitting the Gaussian plume model in both the horizontal and vertical (method 2). The two approaches were in agreement. For all the other flights, only the method of fitting Gaussian profiles in both the horizontal and vertical could be used (method 2), as the mixing was clearly incomplete in the vertical. For one flight, the plume structure was poorly defined due to very low wind speed and the resulting flow rate estimation is considered unreliable.

Overall, the methane flow rate was observed to decrease from around 1 kg s^{-1} in the first few days of the leak to less than 0.5 kg s^{-1} by early May.

6.1.2 Whole Air Samples and Non-methane Hydrocarbons

Air sampling revealed that the Elgin plume was dominated by linear and branched chain alkanes and some monoaromatic compounds. There was a close relationship between CH_4 and NMHC fractions. The presence of very elevated ethane and propane within the plumes was highly indicative of an above sea-surface emission source since these are sub-saturated in seawater and are generally removed to the water column if released at

the seabed. The spatial mixing of higher condensate species with background air was closely related to CH₄ and the C2-C4 NMHCs, indicating that emission to atmosphere was from the point-source leak. The distribution of C1 to C2 – C4 species was found to be consistent with previous published data and with estimates provided by TOTAL. The NMHC data from the FAAM showed no evidence for higher condensate evaporation (e.g. larger >C6 hydrocarbons) into air from the seawater sheen. This would suggest condensate removal was by biological processes in the water.

NMHC concentrations showed a trend towards increasing fractional NMHC content (relative to methane) with time, although there was no significant change in the distribution of NMHCs relative to each other.

6.1.3 HYSPLIT Dispersion Modelling

The NOAA HYSPLIT dispersion model was used to provide estimates of methane concentrations ahead of each flight. This formed the basis of the Safety Management System allowing planning for transects through the plume. Post-event dispersion modelling for the entire period of the leak has generated estimates of the geographical distribution of methane dispersion. Overall, concentrations of methane or other trace gases reaching land were negligible. However, the dispersion modelling does support the suggestion that trace gases could be detected using sensitive instrumentation hundreds of kilometres from the source.

6.2 Lessons learned

The principal lesson learned from this work concerns a considerably increased understanding of the data requirements for accurate and efficient determination of plume flow rates and composition. Specifically concerning the flow rate estimation:

1. More detailed use of pre-flight dispersion modelling and use of forecast or observed (in the few hours before a flight) atmospheric wind and thermodynamic profiles would allow more optimal flight planning. In particular, pre-knowledge of the likelihood of vertical dispersion being capped by an inversion would allow a sampling strategy to be optimised for method 1 or method 2 of §4.3 in advance of the flight. This would allow better use of flight time, enabling repeat sampling to be used to decrease uncertainties.
2. Flights would benefit from a skilled meteorologist on board to interpret boundary-layer structure and recommend variations to the flight plan in real time. Planned upgrades of the aircraft to ground communication of real-time data would reduce but not eliminate this requirement.
3. Experience of developing and optimising the analysis techniques described in this report would allow results to be obtained more quickly in the future.

Concerning the whole air sampling, the principal lesson learned was how to optimise flight manoeuvres in order to efficiently collect samples during rapid passes through a plume. Early use of trace gas data from observatories remote from a leak source, coupled with dispersion modelling, could provide valuable additional information concerning source characteristics.

6.3 Future capability

Experience gained during this incident could potentially accelerate the response to any future event in the following ways:

1. Allow an aircraft Safety Management System to be agreed more quickly.
2. Accelerate the process of flight planning.
3. Accelerate agreement of contractual arrangements (especially if an outline agreement or standby arrangement was already in place).
4. Accelerate post-flight data analysis.

Improvements to any future response could include routine collection and analysis of *in-situ* total-VOC, SO₂, CO, CO₂, H₂S and NO_x data, besides the CH₄ capability demonstrated for the Elgin incident.

Concerning the ability of FAAM and NCAS to respond in the future, there exists a considerable range of possibilities. The FAAM aircraft is usually able to fly on a number of days in excess of 200 per year. However, this is restricted by periods of maintenance (which are generally inflexible) and instrument role changes (which can involve periods when the aircraft is unable to fly or where cancellation of a role change in order to fly would incur considerable cost). The aircraft will typically spend around 10 weeks per year abroad. Return from an

overseas detachment, or delay or cancellation of an overseas detachment, can be particularly expensive (the largest contribution is often the cost of re-scheduling other disrupted work). Whilst at the home base in Cranfield, weekend flying requires greater advance notice than weekday flying and generally incurs considerable additional costs (mainly specified by the airfield and beyond the control of FAAM). An alternative for out-of-hours flying is to temporarily base the aircraft at an airport with 24 hour operation; this also incurs significant cost.

As a result of the above operating constraints, the cost of any pre-agreement to provide a service will depend on the level of service to be guaranteed. A simple agreement to respond on a “best endeavours” basis, as was done for the Elgin incident, would cost only a small fraction of higher levels of guaranteed response. As a guide, the annual cost of the FAAM facility is around £4.5M per year and the cost of associated projects which could potentially be disrupted would typically be several £M.

In principle the FAAM aircraft is able to operate in most parts of the world. The owners and operators restrict operations in regions of high security risk. There are limitations in remote regions arising from the requirements for diversionary airports. This can be severe in polar regions. Currently the aircraft does not have a capability to fly north of 78° but ongoing investment is likely to alleviate this restriction in the near future. Extended periods of operation overseas would carry restrictions arising from FAAM's limited numbers of personnel and their other commitments.

The detailed hydrocarbon analysis presented in this report was completed quickly, generally within 48 hours, since the aircraft was located in reasonable geographic proximity to the main analysis lab in York. Use of the aircraft at short notice overseas would either limit the speed with which non-methane hydrocarbon data could be determined, or would require the overseas deployment of the ground analysis equipment. The latter is possible, indeed is the norm for planned scientific experiments, but incurs cost and relies on staff availability. It can also take significant time to arrange shipping of analysis equipment.

Sampling of the Elgin plume was considerably aided by the fact that the work was entirely over the sea, where obstacles are few, well documented and easily seen during normal daytime conditions. Sampling of a plume over land, especially over complex terrain, would carry considerable additional restrictions. The FAAM aircraft is unable to fly below 500 ft above the highest nearby terrain or obstacles.

For enhancement of longer term measurement capability over complex terrain or in dangerous conditions, FAAM and NCAS are working to develop a UAV capability. However such a capability will have much reduced measurement sophistication than the FAAM aircraft.

7 Acknowledgments

We wish to thank all of the staff of FAAM, NCAS and the Met Office who took part in the Elgin flights. Directflight Ltd, their pilots, cabin crew, ground staff and management consistently provided outstanding support under demanding conditions. BAe Systems support for the use of their aircraft is gratefully acknowledged, as is the cooperation of the Met Office in allowing the use of the shared FAAM facility. Numerous science staff of the National Centre for Atmospheric Science and the Met Office took part in the flights and/or provided post-flight analysis. The work of the legal and management teams at the Natural Environment Research Council HQ in Swindon in managing the contractual arrangements is gratefully acknowledged. Additional contributions to the first two flights were provided by staff and students of Royal Holloway College, London. Advice provided by staff of the NOAA Earth Systems Research Laboratory was of considerable assistance in mission planning and in data interpretation. Additional NCAS staff have proof read this report.

References

- Atkinson, R., 1994: Gas-phase tropospheric chemistry of organic-compounds. *J. Phys. Chem. Ref. Data*, **R1**, R1.
- Baer, D., J. Paul, J. Gupta, and A. O'Keefe, 2002: Sensitive absorption measurements in the near-infrared region using off-axis integrated-cavity-output spectroscopy. *Applied Physics B*, **75**(2-3), 261–265.
- Draxler, R., 1999: HYSPLIT4 user's guide. noaa tech. memo. erl arl-230. Technical report, NOAA Air Resources Laboratory, Silver Spring, MD.
- Draxler, R. and G. Hess, 1997: Description of the HYSPLIT 4 modeling system. NOAA Tech. Memo. ERL ARL-224. Technical report, NOAA Air Resources Laboratory, Silver Spring, MD.
- Draxler, R. and G. Hess, 1998: An overview of the HYSPLIT 4 modeling system of trajectories, dispersion, and deposition. *Aust. Meteor. Mag.*, **47**, 295–308.
- Hallquist, M., J. Wenger, U. Baltensperger, Y. Rudich, D. Simpson, M. Claesys, J. Domment, N. Donahue, C. George, A. Goldstein, J. Hamilton, H. Herrmann, Y. Hoffman, Y. Iinuma, M. Jany, M. Jenkin, J. Jimenez, A. Kiendler-Scharr, et al., 2009: The formation, properties and impact of secondary organic aerosol: current and emerging issues. *Atmos. Chem. & Phys*, **9**, 5155–5236.
- Hopkins, J., C. Jones, and A.C.Lewis, 2011: A dual channel gas chromatograph for atmospheric analysis of volatile organic compounds including oxygenated and monoterpene compounds. *Journal of Environmental Monitoring*, **13**, 2268–2276.
- Hopkins, J., K. Read, and A. Lewis, 2003: A two column method for long-term monitoring of non-methane hydrocarbons (NMHCs) and oxygenated volatile organic compounds. *Journal of Environmental Monitoring*, **5**, 8–13.
- Houweling, S., F. Dentener, and J. Lelieveld, 1998: The impact of non-methane hydrocarbons on tropospheric photochemistry. *J. Geophys. Res.*, **103**, 10673–10696.
- <http://www.class.ngdc.noaa.gov/saa/products/welcome>, 2012: . Website.
- Isaksen, G., 2004: Central north sea hydrocarbon systems: Generation, migration, entrapment, and thermal degradation of oil and gas. *American Association of Petroleum Geologists Bulletin*, **88**, 1545–1572.
- Lidster, R., J. Hamilton, and A. Lewis, 2011: The application of two total transfer valve modulators for comprehensive two-dimensional gas chromatography of volatile organic compounds. *Journal of Separation Science*, **34**, 812–821.
- O'Shea, S. J., S. J.-B. Bauguitte, M. W. Gallagher, D. Lowry, and C. J. Percival, 2013: Development of a cavity enhanced absorption spectrometer for airborne measurements of ch4 and co2. *Atmospheric Measurement Techniques Discussion, in preparation*.
- Paul, J., L. Lapson, and J. Anderson, 2001: Ultrasensitive absorption spectroscopy with a high-finesse optical cavity and off-axis alignment. *Appl. Opt.*, **40**(27), 4904–4910.
- Press, W., S. Teukolsky, W. Vetterling, and B. Flannery, 2007: *Numerical Recipes*. Cambridge University Press.
- Ryerson, T. B., K. C. Aikin, W. M. Angevine, E. Atlas, D. R. Blake, C. A. Brock, F. C. Fehsenfeld, R. S. Gao, J. A. de Gouw, D. W. Fahey, J. S. Holloway, D. A. Lack, R. A. Lueb, S. Meinardi, A. Middlebrook, D. M. Murphy, J. A. Neuman, J. B. Nowak, D. D. Parrish, et al., 2011: Atmospheric emissions from the deepwater horizon spill constrain air-water partitioning, hydrocarbon fate, and leak rate. *Geophys. Res. Lett.*, **38**, doi: 10.1029/2011GL046726.
- Turner, D., 1994: *Workbook of Atmospheric Dispersion Estimates*. Lewis Publishers.